CIVIL ENGINEERING STUDIES
Illinois Center for Transportation Series No. 13-025
UILU-ENG-2013-2026
ISSN: 0197-9191

ULTIMATE PIER AND CONTRACTION SCOUR PREDICTION IN COHESIVE SOILS AT SELECTED BRIDGES IN ILLINOIS

Prepared By
Timothy D. Straub
U.S. Geological Survey

Thomas M. Over
U.S. Geological Survey

Marian M. Domanski
U.S. Geological Survey

Research Report No. FHWA-ICT-13-025

A report of the findings of
ICT-R27-105
Bridge Scour Estimation at Sites with Cohesive Soils

Illinois Center for Transportation

September 2013

1. Report No.	2. Government Accession No.	3. Recipient's Catalog No.
FHWA-ICT-13-025		

4. Title and Subtitle	5. Report Date
Ultimate Pier and Contraction Scour Prediction in Cohesive Soils at Selected Bridges in Illinois	September 2013
	6. Performing Organization Code

7. Author(s)	8. Performing Organization Report No.
Straub, T.D., Over, T.M., Domanski, M.M.	ICT-13-025 UILU-ENG-2013-2026

9. Performing Organization Name and Address	10. Work Unit No. (TRAIS)
Illinois Center for Transportation Department of Civil & Environmental Engineering University of Illinois at Urbana-Champaign 205 N. Mathews Ave., MC-250 Urbana, IL 61801	11. Contract or Grant No. R27-105

12. Sponsoring Agency Name and Address	13. Type of Report and Period Covered
Illinois Department of Transportation Bureau of Materials and Physical Research 120 E. Ash St. Springfield, IL 62704	14. Sponsoring Agency Code

15. Supplementary Notes

16. Abstract

The Scour Rate In COhesive Soils-Erosion Function Apparatus (SRICOS-EFA) method includes an ultimate scour prediction that is the equilibrium maximum pier and contraction scour of cohesive soils over time. The purpose of this report is to present the results of testing the ultimate pier and contraction scour methods for cohesive soils on 30 bridge sites in Illinois. Comparison of the ultimate cohesive and non-cohesive methods, along with the Illinois Department of Transportation (IDOT) cohesive soil reduction-factor method and measured scour are presented. Also, results of the comparison of historic IDOT laboratory and field values of unconfined compressive strength of soils (Q_u) are presented. The unconfined compressive strength is used in both ultimate cohesive and reduction-factor methods, and knowing how the values from field methods compare to the laboratory methods is critical to the informed application of the methods.

On average, the non-cohesive method results predict the highest amount of scour, followed by the reduction-factor method results; and the ultimate cohesive method results predict the lowest amount of scour. The 100-year scour predicted for the ultimate cohesive, non-cohesive, and reduction-factor methods for each bridge site and soil are always larger than observed scour in this study, except 12% of predicted values that are all within 0.4 ft of the observed scour. The ultimate cohesive scour prediction is smaller than the non-cohesive scour prediction method for 78% of bridge sites and soils. Seventy-six percent of the ultimate cohesive predictions show a 45% or greater reduction from the non-cohesive predictions that are over 10 ft. Comparing the ultimate cohesive and reduction-factor 100-year scour predictions methods for each bridge site and soil, the scour predicted by the ultimate cohesive scour prediction method is less than the reduction-factor 100-year scour prediction method for 51% of bridge sites and soils.

Critical shear stress remains a needed parameter in the ultimate scour prediction for cohesive soils. The unconfined soil compressive strength measured by IDOT in the laboratory was found to provide a good prediction of critical shear stress, as measured by using the erosion function apparatus in a previous study. Because laboratory Q_u analyses are time-consuming and expensive, the ability of field-measured Rimac data to estimate unconfined soil strength in the critical shear–soil strength relation was tested. A regression analysis was completed using a historic IDOT dataset containing 366 data pairs of laboratory Q_u and field Rimac measurements from common sites with cohesive soils. The resulting equations provide a point prediction of Q_u, given any Rimac value with the 90% confidence interval. The prediction equations are not significantly different from the identity Q_u = Rimac. The alternative predictions of ultimate cohesive scour presented in this study assume Q_u will be estimated using Rimac measurements that include computed uncertainty. In particular, the ultimate cohesive predicted scour is greater than observed scour for the entire 90% confidence interval range for predicting Q_u at the bridges and soils used in this study, with the exception of the six predicted values that are all within 0.6 ft of the observed scour.

17. Key Words	18. Distribution Statement
Bridge, Pier Contraction, Scour, Cohesive, Soil, Illinois, SRICOS, EFA, HEC-18	No restrictions. This document is available to the public through the National Technical Information Service, Springfield, Virginia 22161

19. Security Classif. (of this report)	20. Security Classif. (of this page)	21. No. of Pages	22. Price
Unclassified	Unclassified	26 plus appendices	N/A

ACKNOWLEDGMENT

This publication is based on the results of ICT R27-105, **Bridge Scour Estimation at Sites with Cohesive Soils**. ICT-R105 was conducted in cooperation with the Illinois Center for Transportation; the Illinois Department of Transportation, Division of Highways; and the U.S. Department of Transportation, Federal Highway Administration.

Members of the Technical Review panel were the following:

Neil VanBebber (Chair), Illinois Department of Transportation

Dan Ghere, Federal Highway Administration

Mark Gawedzinski, Illinois Department of Transportation

Bill Kramer, Illinois Department of Transportation

Dan Brydl, Federal Highway Administration

Riyad Wahab, Illinois Department of Transportation

Matt O'Connor, Illinois Department of Transportation

Veniecy Pearman-Green, Illinois Department of Transportation

Mark Dell, Illinois Department of Transportation

DISCLAIMER

MANUFACTURERS' NAMES

EXECUTIVE SUMMARY

The Scour Rate In COhesive Soils-Erosion Function Apparatus (SRICOS-EFA) method includes an ultimate scour prediction that is the equilibrium maximum pier and contraction scour of cohesive soils over time. The purpose of this report is to present the results of testing the ultimate pier and contraction scour methods for cohesive soils on 30 bridge sites in Illinois. Comparison of the ultimate cohesive and non-cohesive methods, along with the Illinois Department of Transportation (IDOT) cohesive soil reduction-factor method and measured scour are presented. Also, results of the comparison of historic IDOT laboratory and field values of unconfined compressive strength of soils (Q_u) are presented. The unconfined compressive strength is used in both ultimate cohesive and reduction-factor methods, and knowing how the values from field methods compare to the laboratory methods is critical to the informed application of the methods.

On average, the non-cohesive method results predict the highest amount of scour, followed by the reduction-factor method results; and the ultimate cohesive method results predict the lowest amount of scour. The 100-year scour predicted for the ultimate cohesive, non-cohesive, and reduction-factor methods for each bridge site and soil are always larger than observed scour in this study, except 12% of predicted values that are all within 0.4 ft of the observed scour. The ultimate cohesive scour prediction is smaller than the non-cohesive scour prediction method for 78% of bridge sites and soils. Seventy-six percent of the ultimate cohesive predictions show a 45% or greater reduction from the non-cohesive predictions that are over 10 ft. Comparing the ultimate cohesive and reduction-factor 100-year scour predictions methods for each bridge site and soil, the scour predicted by the ultimate cohesive scour prediction method is less than the reduction-factor 100-year scour prediction method for 51% of bridge sites and soils.

Critical shear stress remains a needed parameter in the ultimate scour prediction for cohesive soils. The unconfined soil compressive strength measured by IDOT in the laboratory was found to provide a good prediction of critical shear stress, as measured by using the erosion function apparatus in a previous study. Because laboratory Q_u analyses are time-consuming and expensive, the ability of field-measured Rimac data to estimate unconfined soil strength in the critical shear–soil strength relation was tested. A regression analysis was completed using a historic IDOT dataset containing 366 data pairs of laboratory Q_u and field Rimac measurements from common sites with cohesive soils. The resulting equations provide a point prediction of Q_u, given any Rimac value with the 90% confidence interval. The prediction equations are not significantly different from the identity Q_u = Rimac. The alternative predictions of ultimate cohesive scour presented in this study assume Q_u will be estimated using Rimac measurements that include computed uncertainty. In particular, the ultimate cohesive predicted scour is greater than observed scour for the entire 90% confidence interval range for predicting Q_u at the bridges and soils used in this study, with the exception of the six predicted values that are all within 0.6 ft of the observed scour.

CONTENTS

CHAPTER 1 INTRODUCTION

Most methods of predicting pier and contraction scour at bridges are based on erodibility estimates from non-cohesive soils data, which generally overestimate the scour of cohesive soils, resulting in increased pier depth and cost to design and build bridges. Results from testing a new method of predicting pier and contraction scour in cohesive soils showed promise for application in Illinois (Straub and Over 2010). The scour rate in cohesive soils-erosion function apparatus (SRICOS-EFA) methodology outlined in National Cooperative Highway Research Program (NCHRP) Report 516 (2004) was tested in Illinois at 15 sites (Straub and Over 2010). The method was updated in Briaud et al. (2011), and the update was also included in the Federal Highway Administration (FHWA) Hydraulic Engineering Circular No. 18 (HEC-18) manual (Arneson et al. 2012).

The Straub and Over (2010) study also compared the Illinois Department of Transportation (IDOT) cohesive soil reduction-factor method, which adjusts HEC-18 non-cohesive scour estimates using a reduction factor based on the soil unconfined compressive strength. It was determined that this reduction-factor method may not, by itself, always provide the best estimate of bridge scour, and that computing SRICOS ultimate scour (previously called Zmax) using the unconfined compressive strength of the soil and mean channel hydraulic properties may improve the estimate of scour. The SRICOS ultimate cohesive scour is the equilibrium maximum contraction and pier scour of cohesive soils over time. This “upper limit” of scour prediction, hereafter referred to as the ultimate cohesive method, can be used alongside the IDOT cohesive soil reduction-factor method, hereafter referred to as the reduction-factor method, and the scour prediction method for non-cohesive soils outlined in HEC-18, hereafter referred to as non-cohesive method.

The FHWA review team for the Straub and Over (2010) study agreed with the need for additional research to develop improved procedures for estimating scour in cohesive soils and commented on the need to increase the number of testing sites. To further test the ultimate cohesive method in Illinois, the U.S. Geological Survey (USGS), in cooperation with the Illinois Center for Transportation and IDOT, began a study in 2011 at 15 additional bridge sites throughout the state.

1.1 PURPOSE AND SCOPE

The purpose of this report is to present a comparison of the ultimate cohesive and non-cohesive methods, along with the reduction-factor methods and observed scour. The combined results of the 15 bridge sites in the original study and the 15 additional bridge sites in this study are presented. These results can be used to determine the best estimation of scour, which can reduce the costs for design and construction of new bridge foundations and also reduce the number of previously categorized scour-critical bridges that require a plan of action.

Also, results of the comparison of historic IDOT laboratory and field values of unconfined compressive strength are presented. The evaluation of the field-determined value is critical in determining the reliability of the ultimate cohesive and reduction-factor methods.

1.2 PREVIOUS STUDIES

The SRICOS-EFA methodology as outlined in NCHRP Report 516 (2004) documents the development and validation of the SRICOS-EFA methodology with laboratory testing, numerical modeling, and field data from eight bridges with cohesive soils in Texas. The method

is evaluated by comparing predicted scour depths and measured scour depths for ten piers at eight bridges. Briaud has collaborated on a number of additional papers involving the SRICOS-EFA methodology, including Briaud et al. (2004), Briaud and Chen (2005), and Brandimarte et al. (2006). The method was updated in Briaud et al. (2011), and the update was also included in the Federal Highway Administration Hydraulic Engineering Circular No. 18 (Arneson et. al. 2012).

Additional testing of the SRICOS-EFA methodology has been conducted at two sites in Alabama (Curry et al. 2003), five sites in Maryland (Ghelardi 2004), and three sites in South Dakota (Ting et al. 2010). Similar laboratory and field testing was done in Georgia (Sturm et al. 2004). A detailed summary of each study was included in Ting et al. (2010).

1.3 SITE SELECTION

Sites were submitted from the nine IDOT districts for consideration in the study. The sites were identified by a two-number system (e.g., 1-1). The first number represents the IDOT district, and the second number is the order in which they were submitted for selection. The final 30 bridge sites selected for testing are shown in Figure 1 and Table 1. The 15 sites added to this study that were not in the original study (Straub and Over 2010) are 1-5, 1-8, 3-13, 3-15, 3-34, 5-3, 5-21, 5-24, 5-25, 5-26, 5-27, 5-31, 7-31, 7-32, and 8-82. The selection of sites for this study was based on the availability of design plans and the existence of historic soil-boring data indicating cohesive soil at and below the interface of the streambed and pier.

1.4 APPROACH

Data from the original 15 sites (Straub and Over, 2010) were used to recalculate pier and contraction scour using the updated ultimate cohesive methods outlined in Briaud et al. (2011) and Arneson et al. (2012). The 15 additional sites were modeled and scour depths calculated using the ultimate cohesive and non-cohesive methods, along with the reduction-factor method. The predicted scour results were then compared to measured scour data. Scour data was collected using echo sounder, ground penetrating radar (GPR), digital level, manual probing, and/or a survey-grade global positioning system (GPS), depending on the site conditions.

The hydraulic parameters for the ultimate cohesive methods were obtained from Hydrologic Engineering Center River Analysis System (HEC-RAS) models (U.S. Army Corps of Engineers 2010). If HEC-RAS models were not available for the sites, pre-existing hydraulic models obtained from the IDOT districts or raw survey data were converted to HEC-RAS models. HEC-RAS also was used to perform the non-cohesive bridge scour analysis.

For the ultimate cohesive methods, the soil parameter (critical shear stress) was determined from the relation developed in Straub and Over (2010), which requires input of laboratory unconfined compressive strength value, Q_u. Because field Q_u values are also used in practice as well as in this study, an evaluation of past IDOT laboratory and field Q_u values was completed.

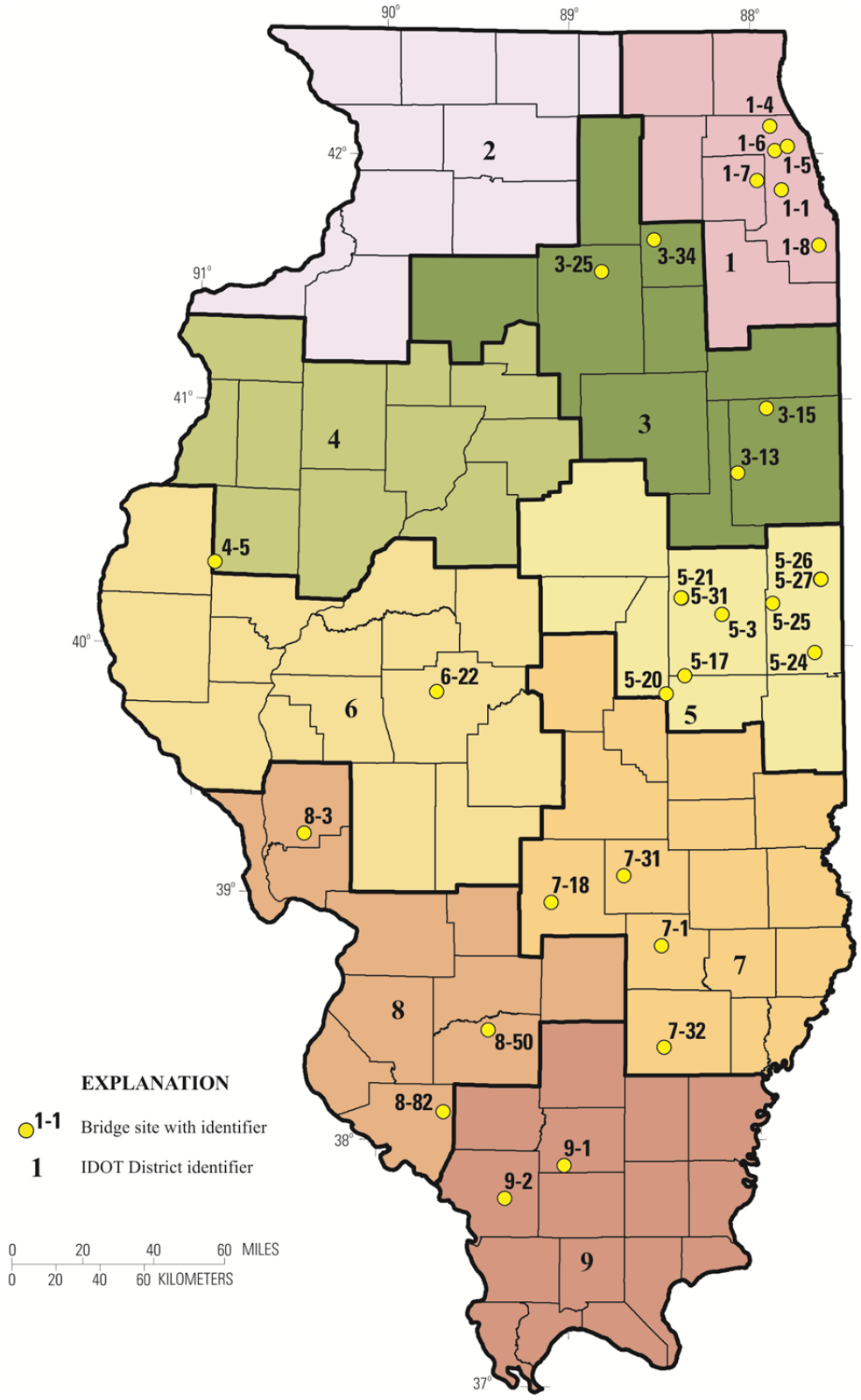

Figure 1. Location of the 30 bridge sites selected for scour prediction analysis in Illinois.

Table 1. Bridge Site Identifier, Structure Number, Location, Drainage Area, Feature Crossed, Pre-Existing Hydraulic Model Information for the 30 Bridge Sites Selected for Scour Prediction Analysis

[latitude and longitude (decimal degree) are referenced to WGS84; mi^2, square miles; — indicates no pre-existing model]

Bridge Site Identifier	Structure Number	Location	County	Feature Crossed	Latitude	Longitude	Drainage Area (mi^2)	Pre-Existing Hydraulic Model
1-1	016-0634	Cermak Road	Cook	Des Plaines River	41.849769	-87.827486	484	HEC-2
1-4	016-0273	Palatine Road	Cook	Des Plaines River	42.108642	-87.887533	359	HEC-2
1-5	016-0555	Oakton Street	Cook	N. Br. Chicago River	42.026428	-87.791650	96	HEC-2
1-6	016-0829	Touhy Avenue	Cook	Des Plaines River	42.010300	-87.861250	416	HEC-2
1-7	022-0045	IL 83	Du Page	Salt Creek	41.889169	-87.961886	91	FEQ
1-8	016-0954	IL 83	Cook	Little Calumet	41.622619	-87.627731	232	HEC-RAS
3-13	038-0207	US 54	Iroquois	Tributary to Spring Creek	40.701203	-88.083503	37	WSPRO
3-15	038-0185	US 45	Iroquois	Langan Creek	40.963372	-87.923417	83	HEC-RAS
3-25	050-0159	IL 23	La Salle	Indian Creek	41.523164	-88.816189	135	WSPRO
3-34	047-3133	Hale Road	Kendall	Big Rock Creek	41.652078	-88.528858	117	Survey
4-5	055-0010	IL 61	McDonough	Lamoine River	40.330822	-90.896167	655	HEC-RAS
5-3	010-4099	Perkins Road	Champaign	Saline Branch	40.127583	-88.174294	72	—
5-17	021-4022	CR 1550N	Douglas	Kaskaskia River	39.879292	-88.376447	109	—
5-20	074-0034	CR 100N	Piatt	Lake Fork	39.806381	-88.476378	149	—
5-21	010-0017	I-74	Champaign	Sangamon River	40.195461	-88.391703	364	WSPRO
5-24	092-0169	CH 23	Vermilion	Fairview Creek	39.968503	-87.680836	10	WSPRO
5-25	092-0171	IL 49	Vermilion	Tributary to Stony Creek	40.170592	-87.903569	12	HEC-RAS
5-26	092-0172	CH 15	Vermilion	W. Br. N. Fork Vermilion River	40.265758	-87.644425	6	WSPRO
5-27	092-0173	CH 15	Vermilion	North Fork Vermilion River	40.265733	-87.642714	267	WSPRO
5-31	010-0016	I-74	Champaign	Sangamon River	40.195661	-88.392114	364	WSPRO
6-22	084-0180	IL 97	Sangamon	Spring Creek	39.814914	-89.699717	107	WSPRO
7-1	013-0010	US 45	Clay	Little Wabash River	38.783661	-88.508028	711	—
7-18	026-0034	US 51	Fayette	Kaskaskia River	38.960397	-89.088142	1,940	WSPRO
7-31	025-2008	US 40	Effingham	Second Creek	39.068511	-88.704056	6	HEC-RAS
7-32	096-0007	IL 15	Wayne	Dry Fork	38.371181	-88.498094	61	HEC-RAS
8-3	031-0022	US 67	Greene	Macoupin Creek	39.234383	-90.394606	868	HEC-2
8-50	095-0066	IL 177	Washington	Little Crooked Creek	38.441681	-89.416667	84	HEC-2
8-82	079-0041	IL 154	Randolph	Marys River	38.108392	-89.649589	18	WSPRO
9-1	028-0037	IL 149	Franklin	Big Muddy River	37.891544	-89.019572	795	WSPRO
9-2	039-0036	IL 127	Jackson	Big Muddy River	37.757994	-89.327622	2,162	WSPRO

CHAPTER 2 HYDRAULICS

2.1 BRIDGE AND CHANNEL GEOMETRY DATA

As part of the site selection process, the IDOT districts submitted any available hydraulic models and plan data. The pre-existing hydraulic model types and formats are listed in Table 1. Additional data about the bridge structure (e.g., widths, lengths and shapes, skew angle, Manning's coefficient, and channel slope) also were collected if data were not available from the pre-existing hydraulic models or plans. USGS personnel collected data with echo sounder, ground penetrating radar (GPR), digital level, manual probing, and/or a survey-grade global positioning system (GPS) to document current channel conditions at the 30 sites.

2.2 MODELING

Pre-existing models obtained from the IDOT districts (Table 1) were converted to HEC-RAS models. For the majority of the sites, 100- and 500-year flood magnitudes were obtained from Soong et al. (2004) or StreamStats (http://streamstats.usgs.gov), which uses equations developed in Soong et al. (2004) for ungaged rural sites in Illinois. At the following sites, the 100- and 500-year flows from the pre-existing models were used because of urban influences or channel and watershed modifications: 1-1, 1-4, 1-5, 1-6, 1-8, 5-25, and 7-32. The majority of the original 15 sites were near stream gages, and the models were calibrated to the gage data, and the other sites only modeled the existing or new channel and bridge information. The HEC-RAS models were used to perform the HEC-18 non-cohesive bridge scour analysis (in the Hydraulic Design tab), and obtain the hydraulic parameters needed to perform the ultimate cohesive scour analysis, as described in the Scour section.

CHAPTER 3 SOILS

For the ultimate cohesive pier and contraction methods, critical shear stress is needed. In Straub and Over (2010), the following soil properties were determined from material in the Shelby-tube samples from the sites and were used to attempt to correlate with critical shear: liquid limit, plastic limit, plasticity index, moisture content, unconfined compressive strength (Q_u), wet density, particle-size distribution, mean diameter, percent sand, percent silt, percent clay. The best relation was obtained using the laboratory unconfined compressive strength value Q_u, and the following section describes the analysis in Straub and Over (2010). Also, because field Q_u values are used in practice as well as in this study, an evaluation of past IDOT laboratory and field Q_u values was completed and described in the unconfined compressive strength and Rimac report section.

3.1 UNCONFINED COMPRESSIVE STRENGTH AND CRITICAL SHEAR STRESS

The data and results of the regression of laboratory Q_u and critical shear stress from Straub and Over (2010) are presented in Figure 2 and Table 2. The laboratory tests were performed on undisturbed cohesive sediment in standard Shelby tubes with a 3-in. (76.2-mm) outside diameter. All erosion laboratory tests were performed by the IDOT in their erosion function apparatus (EFA) and shear values calculated as outlined in (NCHRP 2004; Straub and Over 2010). The Q_u tests were also performed by IDOT, using calibrated laboratory equipment, according to AASHTO T 208 / ASTM D 2166. The compression machine was a Soiltest model U-600 with a 1,000-lb capacity. The device is capable of variable plate speeds from zero to 0.25 in. per minute. Load measurements were obtained by calibrated/verified proving rings. The uniform area correction was used in the stress calculations. The NCHRP Report 516 (2004) notes Flaxman's (1963) study of the evaluation of the boundary between eroding and non-eroding channel flows utilizing unconfined compressive strength of cohesive soils (also referenced and used by Ivarson, 1998). NCHRP Report 516 (2004) also presents data from 91 EFA tests and states that no relationship could be found between critical shear stress and common soil properties (properties include undrained shear strength). To help determine whether the relation between Q_u and critical shear stress presented in Figure 2 is applicable to a given soil, additional soil parameters are presented in Table 2.

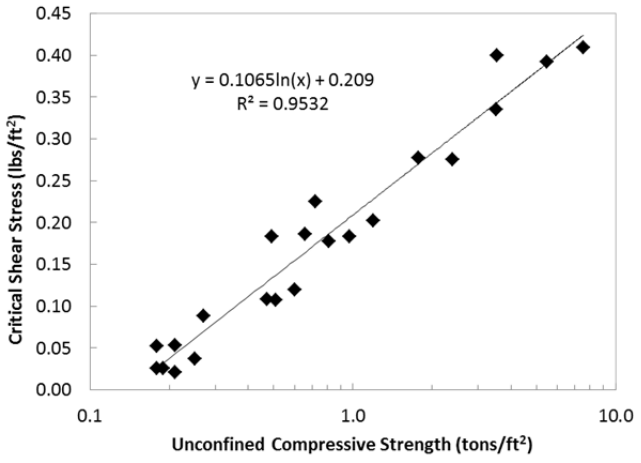

Figure 2. Best-fit natural logarithm functions of critical shear stress and unconfined compressive strength for samples obtained in Straub and Over (2010).

Table 2. Critical Shear Stress and Unconfined Compressive Strength and Additional Soil Parameter Values for Samples Obtained in Straub and Over (2010).

Sample	Soil Classification AASHTO	Soil Classification IDOT	Wet Density lb/ft^3	Percent Moisture Content	Unconfined Compressive Strength (tons/ft^2)	Critical Shear Stress (lb/ft^2)	Liquid Limit	Plastic Limit	Plasticity Index	Mean Particle Size (D_{50}) mm	Percent Gravel	Percent Sand	Percent Silt	Percent Clay
1-1 Soil 1	A-7-5(29)	Silty Clay	104.2	45.0	0.27	0.0888	59	34	25	0.0041	0.5	18.2	54.5	20.9
1-4 Soil 1	A-6 (02)	Sand Loam	133.3	19.8	2.39	0.2757	28	17	11	0.0148	30.4	16.3	46.8	32.1
1-4 Soil 2	A-4 (2)	Silt Loam	142.0	17.3	0.19	0.0257	21	16	5	0.0100	0.8	32.4	29.7	16.4
1-4 Soil 3	A-4 (3)	Clay Loam	135.3	15.1	3.52	0.3352	23	15	8	0.0217	13.9	32.9	36.2	15.9
1-4 Soil 4	A-4 (3)	Silty Clay-Loam	139.4	16.7	1.78	0.2774	22	15	7	0.0149	6.4	37.7	41.2	16.5
1-6 Soil 1	A-7-6(20)	Clay	112.7	35.7	0.18	0.0257	51	27	24	0.0084	4.8	15.0	61.5	23.5
1-7 Soil 1	A-6 (02)	Sand Loam	130.9	21.1	0.72	0.2256	33	21	12	0.1296	21.5	14.7	65.0	20.3
1-7 Soil 2	A-4 (2)	Loam	119.8	23.4	0.60	0.1199	27	18	9	0.0679	15.0	31.0	38.8	22.4
3-25 Soil 1	A-4 (0)	Loam	140.3	10.4	1.20	0.2026	17	13	4	0.0591	4.6	30.7	42.1	20.9
4-5 Soil 1	A-6 (09)	Silty-Clay Loam	118.8	29.2	0.21	0.0207	32	20	12	0.0148	0.0	12.0	65.6	21.5
4-5 Soil 2	A-4 (8)	Silty-Clay Loam	123.2	27.0	0.66	0.1859	30	20	10	0.0204	0.0	31.3	46.1	18.1
5-17 Soil 1	A-4 (1)	Clay Loam	143.0	11.7	5.47	0.3924	21	14	7	0.0213	7.8	31.4	48.7	18.7
5-20 Soil 1	A-4 (3)	Clay Loam	140.1	13.4	3.53	0.3995	24	15	9	0.0274	6.3	32.0	42.7	18.7
6-22 Soil 1	A-4 (8)	Silty-Clay Loam	119.5	20.2	0.97	0.1838	33	22	11	0.0167	0.9	4.0	66.9	29.0
7-1 Soil 1	A-4 (4)	Loam	118.6	23.6	0.21	0.0535	27	17	10	0.0331	4.5	6.3	68.2	25.4
7-1 Soil 2	A-4 (3)	Loam	119.0	23.1	0.25	0.0370	25	17	8	0.0304	1.2	29.1	49.8	21.1
7-18 Soil 1	A-4 (1)	Loam (Till)	143.1	9.8	7.53	0.4089	19	13	6	0.0345	6.6	6.2	68.8	25.0
8-3 Soil 1	A-6 (17)	Silty-Clay Loam	119.7	23.5	0.81	0.1775	38	21	17	0.0095	0.1	4.8	70.2	25.0
8-50 Soil 1	A-6 (10)	Silty Clay-Loam	121.1	24.1	0.51	0.1076	30	18	12	0.0105	0.1	18.2	54.5	20.9
9-1 Soil 1	A-6 (06)	Clay Loam	125.5	24.9	0.18	0.0522	28	16	12	0.0314	0.0	16.3	46.8	32.1
9-2 Soil 1	A-6 (12)	Silty Clay-Loam	118.0	23.7	0.47	0.1086	33	19	14	0.0173	0.0	32.4	29.7	16.4
9-2 Soil 2	A-6 (14)	Silty Clay-Loam	118.5	21.3	0.49	0.1838	34	19	15	0.0171	0.0	32.9	36.2	15.9
Maximum			143.1	45.0	7.5	0.4089	59	34	25	0.1296	30.4	37.7	75.2	39.6
Minimum			104.2	9.8	0.2	0.0207	17	13	4	0.0041	0.0	4.0	29.7	15.8
Median			122.2	22.2	0.6	0.1807	28	17	11	0.0189	2.9	18.1	49.3	21.0
Average			126.6	21.8	1.5	0.1767	29	18	11	0.0280	5.7	19.9	52.3	22.2
Standard Deviation			11.2	8.1	1.9	0.1270	9.9	4.8	5.3	0.0275	8.0	11.5	13.5	5.7

3.2 UNCONFINED COMPRESSIVE STRENGTH AND RIMAC

Samples, analyses, and results discussed above from Straub and Over (2010), show that the Q_u, as measured by IDOT in the laboratory, was found to provide a good prediction of critical shear stress (Figure 2). The critical shear was measured by using the erosion function apparatus (EFA). Critical shear stress remains a needed parameter in the ultimate scour prediction for cohesive soils. Because laboratory Q_u analyses are time-consuming and expensive, the ability of field-measured Rimac data to estimate unconfined compressive strength of soil was tested. A Rimac spring tester is an unconfined compression testing device using split spoon samples.

To complete this analysis, an IDOT historic dataset was used containing 366 data pairs of laboratory Q_u and Rimac measurements from sites in Illinois. The plots and associated statistical analyses of these data are included in this report as Appendix A. The numerical data and textural classification on which these plots were based could not be recovered. The USGS therefore digitized the data pairs from the plots to obtain a dataset with 325 total paired Q_u and Rimac values. A comparison of the original and digitized data pairs from the plots is provided in Appendix A, along with a description of the soils and further discussion of the scatter.

There is significant scatter in the plots showing the Rimac and Q_u soil strength estimates. These differences arise from many sources, of which the testing procedure is only one. The paired Q_u and Rimac values come from common sites, but they are from different soil samples obtained using different samplers. Along with the numerical and textural data not being retrieved, the location and timing of each sample could not be retrieved; and it is assumed that at least some of the paired data could have been taken at different locations within the site and possibly at different times.

The proposed Rimac-Q_u relation is shown in Figure 3. It is composed of a combination of two equations and their prediction intervals, one coming from a linear fit to the smaller Rimac and Q_u values after log-transformation and the other from a linear fit to the larger Rimac and Q_u values without transformation. As can be seen from the plots, the prediction interval resulting from the log-transformation for the smaller values accounts for the growth in scatter (heteroscedasticity) as the Rimac and Q_u values increase from zero; whereas for larger values, the prediction interval resulting from the linear fit without transformation accounts for the fact that the scatter has become relatively constant (homoscedastic). Further details of the method of computation of the Rimac-Qu relation are provided in Appendix B.

The point prediction (the solid line near the center of the points in the plots) is given by the following equations:

$$Q_u = 1.0122*\text{Rimac} - 0.0993 \text{ for Rimac} > 1.06 \quad (1)$$

and

$$Q_u = 0.9222*\text{Rimac}^{0.8782} \text{ for Rimac} < 1.06 \quad (2)$$

The values of these coefficients and their confidence intervals are given in Table 3. Notice that at the 5% significance level, the untransformed slope is not significantly different from a value of 1, the untransformed intercept is not significantly different from a value of 0, the log-log slope is not significantly different from a value of 1 (though the upper end of the 95% confidence interval is just a little larger than a value of 1), and the log-log intercept is

not significantly different from a value of 0. These findings mean that neither equation is significantly different from the identity Q_u = Rimac.

At Rimac = 1.06, the two equations give approximately the same value. From equation (1),

$Q_u = 1.0122*1.06 – 0.0993 = 0.9737$,

and from equation (2),

$Q_u = 0.9222*Rimac^{0.8782} = 0.9707$.

The precise intersection of the two regression lines is at Rimac = 1.045525, where Q_u = 0.959000; but because there are Rimac data values between 1.06 and 1.045525, a pair of equations with slightly different coefficients applies at the latter value of Rimac, and so the equations (1) and (2) are not applicable at that Rimac value. The approximate agreement at Rimac = 1.06 was therefore deemed sufficiently accurate.

Table 3. Results of Regression of Q_u Versus Rimac for 325 Data Pairs from Bridge sites in Illinois.

[N, number of data points; tsf, tons per square foot; CI, confidence interval; SE, standard error]

Transformation	Range of Rimac values (tsf)	N	Slope	95% CI of slope	Intercept	95% CI of intercept	Regression SE	Sum of Rimac squares (SS_x)	Rimac mean
None	Rimac > 1.06	130	1.0122	(0.8623, 1.1883)	-0.0993	(-0.4546, 0.2560)	1.0911	122.02	1.8447
log-log	Rimac < 1.06	195	0.8782	(0.7658, 1.0071)	-0.0810	(-0.2468, 0.0848)	0.9323	145.43	0.5705

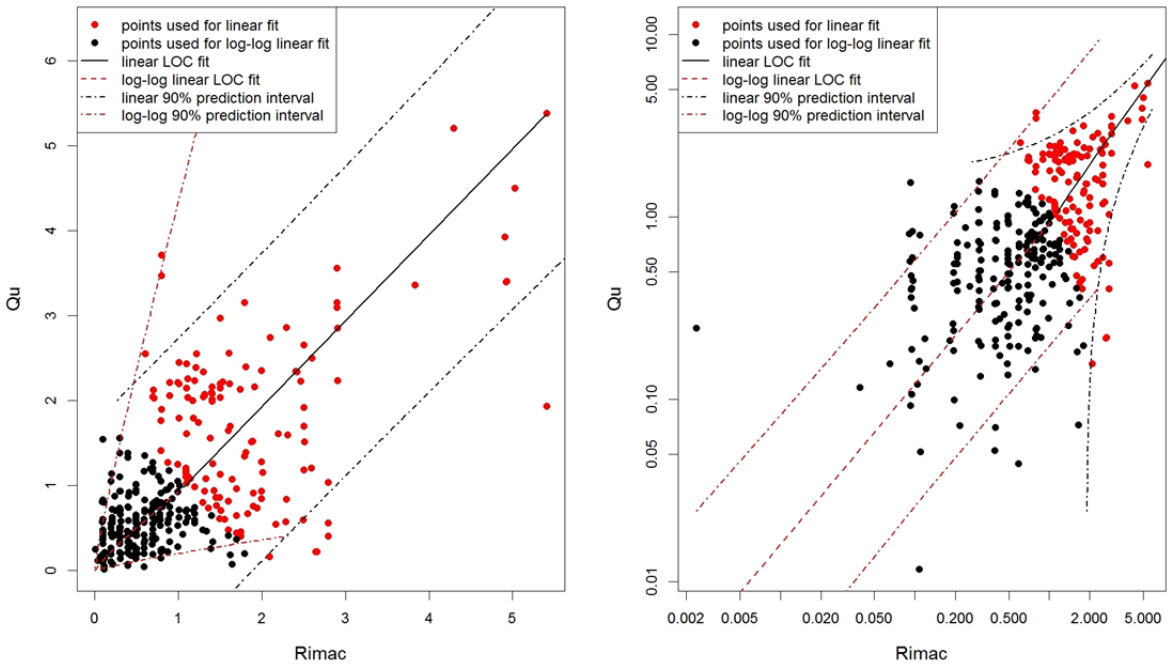

Figure 3. Proposed Rimac-Q_u relation with approximate 90% confidence intervals plotted with linear axes (left), log-log axes (right).

CHAPTER 4 SCOUR

This section presents measured historic scour, brief methods for each scour prediction type, comparison of results, and a reduction-factor approach based on a cohesive soil property. The results include the original 15 sites from Straub and Over (2010) and the 15 sites added during this study. The values for the variables used in scour prediction are presented in Appendix C and provides the range of the typical data used in the analysis.

4.1 MEASURED HISTORIC SCOUR

Scour holes may be filled on the recession limb of hydrographs or during low-flow conditions, causing the elevation of the stream channel bed to be a possibly inaccurate measure of the actual historic scour elevation. To better measure the historic scour, ground penetrating radar (GPR), manual probing, level or GPS survey, and/or echo sounder data were collected by USGS personnel at the 30 sites in Table 4. At sites where the GPR was not usable, a combination of manual probing, and level or GPS survey were used. At one site, echo sounder data were used, which only reflects the stream channel bed at the time of the survey. The accuracy of the GPR is +/- 3 inches, and the other instruments accuracy are within an inch. Additionally at all 30 sites, uncertainty in the measured scour value can be attributed to the placement of historic bridges, construction disturbance, quality of historic cross sections, debris buildup near the bridge, measurement error, and overall channel stability. Regardless, the measured scour data can be compared to predicted scour to evaluate the relative differences in the various scour prediction methods. Scour measurements were taken in the cross sections immediately upstream and downstream of the pier and along the streamwise direction of the pier. The measurements for the original 15 sites were made in 2005, and the additional 15 sites were made in 2012. The measured scour value at each bridge and the technique used to obtain that value are presented in Table 4. At 24 of the 30 sites, at least one pier was in the water at low flow in the main channel, and the pier in the main channel with the maximum pier and contraction scour was chosen for analysis. At the remaining six sites, the piers were perched in the overbank out of the low flow, and the pier in the overbank with the maximum pier and contraction scour was chosen for analysis. The maximum scour occurred mostly at the upstream side of the pier, but at some bridges maximum scour occurred at the downstream side of the pier or cross section or along the pier in the streamwise direction. The scour elevations were compared to historic cross-section elevations to compute the depth of historic scour.

Although scour of cohesive soils occurs over time and not in a single large storm event (as in non-cohesive soils), there is still some value in determining the maximum historic flood that has occurred at each site. The maximum historic flood at the streamgage (Soong et. al. 2004) that is located at or nearby each bridge is presented in Table 4. Both the maximum for the current substructure life and streamgage period of record are listed. The maximum for the period of record is listed because it was noted that previous historic bridges were present at all sites, and current contraction and possibly pier scour measurements may reflect scour that occurred before the current substructure was built. Using the maximum for the streamgage period of record may not fully represent all historic scour because bridges were most likely built before the streamgages were installed. Even with that consideration, all the current substructures at the bridge sites, except site 9-1, have experienced a large flow, which for practical purposes, was arbitrarily defined by Benedict (2003) as any flow that equals or exceeds 70% of the 100-year flow magnitude (Table 4).

Table 4. Measured Scour and Technique Used for Each Bridge Site, and Maximum Historic Flood at a Nearby USGS Streamgage
[---, maximum peak flow for substructure life is the same as the maximum peak flow for period of record]

Bridge Site Identifier	Measured Pier and Contraction Scour (ft)	Technique Used	Year Bridge Substructure Built, Rebuilt, or Modified	Streamgage Used for Maximum Historic Flood	Peak Flow Period of Record Used	Maximum Peak Flow (ft^3/s)				Streamgage 100-yr Flood Estimate (ft^3/s)	Percent Difference Between Peak Flow and 100-yr Flood	
						Period of Record		Substructure Life			Period of Record	Substructure (current) Life
						Date	Flow	Date	Flow			
1-1	2.6	Ground Penetrating Radar	1956	05532500	1914–2005	8/15/1987	9,770	---	---	7,767	26	26
1-4	2.2	Manual Probe	1965	05529000	1941–2005	7/4/1938	5,000	10/1/1986	4,900	7,339	-32	-33
1-5	4.0	Probe	1984	05536000	1951–2012	9/13/2008	3,340	---	---	2,500	34	34
1-6	1.6	Ground Penetrating Radar	1955	05529000	1941–2005	7/4/1938	5,000	10/1/1986	4,900	7,407	-32	-34
1-7	2.3	Manual Probe	1982	05531500	1946–2005	8/17/1987	3,540	---	---	2,820	26	26
1-8	0.3	Probe	1984	05536290	1947–2012	4/6/1947	4,760	11/28/1990	4,150	5,200	-8	-20
3-13	1.4	Survey (pier out of water)	2000	05525500	1948–2012	2/21/1951	22,900	1/8/2008	19,700	26,900	-15	-27
3-15	1.9	Probe	2006	05525500	1948–2012	2/21/1951	22,900	1/8/2008	19,700	26,900	-15	-27
3-25	1.9	Ground Penetrating Radar	1971	05551700	1961–2005	7/18/1996	5,510	---	---	2,850	93	93
3-34	2.1	Ground Penetrating Radar	1990	05551700	1961–2012	7/18/1996	5,510	---	---	2,850	93	93
4-5	6.4	Ground Penetrating Radar	1976	05584500	1945–2005	3/5/1985	38,900	---	---	41,300	-6	-6
5-3	1.6	Manual Probe	1977	03337000	1948–2012	8/12/1993	944	---	---	1,150	-18	-18
5-17	1.2	Ground Penetrating Radar	1981	05591200	1970–2005	5/13/2002	11,000	---	---	12,700	-13	-13
5-20	0.2	Survey (pier out of water)	1963	05590800	1973–2005	3/5/1979	4,030	---	---	4,650	-13	-13
5-21	1.8	Manual Probe	1997	05570910	1978–2012	4/12/1994	13,000	1/14/2005	9,850	14,800	-12	-33
5-24	2.6	Manual Probe	1974	03343400	1960–2012	4/12/1994	8,040	---	---	8,630	-7	-7
5-25	2.2	Survey	1975	03337000	1948–2012	8/12/1993	944	---	---	1,150	-18	-18
5-26	1.2	Survey (pier out of water)	1975	03339000	1914–2012	3/13/1939	48,700	4/13/1994	47,900	45,200	8	6
5-27	2.2	Manual Probe	1975	03339000	1914–2012	3/13/1939	48,700	4/13/1994	47,900	45,200	8	6
5-31	1.5	Manual Probe	1997	05570910	1978–2012	4/12/1994	13,000	1/14/2005	9,850	14,800	-12	-33
6-22	1.4	Survey (pier out of water)	1977	05577500	1948–2005	5/8/1996	10,700	---	---	14,300	-25	-25
7-1	10.8	Ground Penetrating Radar	1966	03379500	1915–2005	1/5/1950	47,000	5/19/1995	43,700	61,100	-23	-28
7-18	2.6	Ground Penetrating Radar	1962	05592500	1922–2005	6/29/1957	62,700	5/13/2002	41,000	60,500	4	-32
7-31	3.9	Manual Probe	1951	03346000	1940–2012	6/7/2008	46,200	---	---	33,100	40	40
7-32	3.0	Manual Probe	1957	03380500	1909–2012	5/17/1990	59,400	---	---	47,600	25	25
8-3	5.4	Manual Probe	1968	05587000	1941–2005	4/12/1994	40,100	---	---	40,700	-1	-1
8-50	3.0	Survey (pier out of water)	1979	05593575	1968–2005	5/17/1995	11,900	---	---	17,600	-32	-32
8-82	1.9	Survey (pier out of water)	1994	05595200	1969–2012	4/29/1996	23,400	---	---	22,000	6	6
9-1	3.5	Ground Penetrating Radar	1987	05597000	1915–2005	5/10/1961	42,900	5/1/1996	14,200	28,100	53	-49
9-2	5.1	Echo sounder	1984	05599500	1931–2005	5/2/1996	33,800	---	---	42,800	-21	-21

4.2 ULTIMATE PIER SCOUR AND CONTRACTION SCOUR IN COHESIVE SOILS

The SRICOS-EFA methodology outlined in NCHRP Report 24-15 (2004) and updated in Briaud et al. (2011) for ultimate scour prediction is presented in this section. The contents are primarily excerpts from the updated version, which is also included in the HEC-18 manual (Arneson, et al. 2012). The methods discussed are used to calculate ultimate pier and contraction scour as denoted in the following equation.

$$y_s = y_{s(cont)} + y_{s(pier)}$$

y_s = ultimate scour (ft, m)

$y_{s(cont)}$ = ultimate contraction scour (ft, m)

$y_{s(pier)}$ = ultimate pier scour (ft, m)

The ultimate scour is the equilibrium maximum contraction and pier scour of cohesive soils over time (i.e., “upper limit” of scour prediction). A schematic for the bridge and hydraulic parameters used is presented in Figure 4. The integrated approach that considers a time factor (scour prediction utilizing time-series data) is not discussed in the section and not used in this study.

4.2.1 Contraction Scour Equations

The ultimate contraction scour can be calculated using the following equations and parameters.

$$y_{s(cont)} = 0.94 y_1 \left(\frac{1.83 V_2}{\sqrt{g y_1}} - \frac{K_u \sqrt{\frac{\tau_c}{\rho}}}{g n y_1^{1/3}} \right)$$

y_1 = Upstream average flow depth (also referred to as the main channel depth at the approach section) (ft, m)

V_2 = Average velocity in the contracted section (at the location of the pier, assuming that the bridge piers are not there) (ft/s, m/s)

τ_c = Critical shear stress of the material (lb/ft^2, N/m^2)

n = Manning’s n

K_u = 1.486 for U.S. Customary units and 1.0 for S.I.

ρ = Density of water (slugs/ft^3, kg/m^3)

g = Acceleration of gravity (ft/s^2, m/s^2)

$$\tau = \gamma \left(\frac{V_2 n}{K_u}\right)^2 {y_0}^{-1/3}$$

τ = Shear stress (lb/ft^2, N/m^2)

γ = Specific weight of water (lb/ft^3, N/m^3)

y_0 = Existing depth of flow in the contracted bridge section before scour (ft, m)

If the shear stress does not exceed the critical value for that material (obtained from test data, a figure such as Figure 2 in this report, or Figure 6.11 in Arneson et al. [2012]), then no contraction scour will occur for the corresponding flow.

Example Problem 1

Given:

Upstream average flow depth (y_1) = 10.80 ft

Existing depth in the contracted section before scour (y_0) = 11.02 ft

Average velocity in the contracted section (V_2) = 5.57 ft/s

Unconfined compressive strength (Q_u) = 6.38 tsf

Manning's n = 0.035

K_u = 1.486

Determine:

The magnitude of the ultimate contraction scour.

Solution:

1. Find the critical shear stress (τ_c)

$$\tau_c = 0.1065 \ln Q_u + 0.209 = 0.1065 \ln 6.38 + 0.209 = 0.406 \text{ psf}$$

2. Compute the initial shear stress (τ)

$$\tau = \gamma \left(\frac{V_2 n}{K_u}\right)^2 {y_0}^{-1/3} = 62.4 \left(\frac{5.57 \times 0.035}{1.486}\right)^2 11.02^{-1/3} = 0.483 \text{ psf}$$

   Because the initial shear stress is greater than the critical shear stress, contraction scour will occur and will be calculated.

3. Compute the contraction scour

$$y_{s(cont)} = 0.94 y_1 \left(\frac{1.83 V_2}{\sqrt{g y_1}} - \frac{K_u \sqrt{\frac{\tau_c}{\rho}}}{g n y_1^{1/3}}\right)$$

$$= 0.94 \times 10.80 \left(\frac{1.83 \times 5.57}{\sqrt{32.2 \times 10.80}} - \frac{1.486 \sqrt{\frac{0.406}{1.938}}}{32.2 \times 0.035 \times 10.80^{1/3}}\right) = 2.78 \text{ ft}$$

Example Problem 2

Given:

Upstream average flow depth (y_1) = 22.6 ft

Existing depth in the contracted section before scour (y_0) = 20.1 ft

Average velocity in the contracted section (V_2) = 3.93 ft/s

Unconfined compressive strength (Q_u) = 5.16 tsf

Manning's n = 0.045

K_u = 1.486

Determine:

The magnitude of the ultimate contraction scour.

Solution:

1. Find the critical shear stress (τ_c)

$$\tau_c = 0.1065 \ln Q_u + 0.209 = 0.1065 \ln 5.16 + 0.209 = 0.384 \text{ psf}$$

2. Compute the initial shear stress (τ)

$$\tau = \gamma \left(\frac{V_2 n}{K_u}\right)^2 {y_0}^{-1/3} = 62.4 \left(\frac{3.93 \times 0.045}{1.486}\right)^2 20.1^{-1/3} = 0.325 \text{ psf}$$

Because the initial shear stress is less than the critical shear stress, contraction scour will not be calculated.

4.2.2 Pier Scour Equations

The ultimate pier scour can be calculated using the following equations and parameters. If the critical velocity does not exceed the critical value for that material (from test data, a figure such as Figure 2 in this report, or Figure 6.11 in Arneson et al. [2012]), then no pier scour will be predicted for the corresponding flow.

$$y_{s(pier)} = 2.2 K_1 K_2 a^{0.65} \left(\frac{2.6 V_p - V_c}{\sqrt{g}}\right)^{0.7}$$

a = Pier width, (ft, m)

V_p = Mean velocity of flow directly upstream of the pier, (ft/s, m/s)

K_1 = Correction factor for pier nose shape

Shape of Pier Nose	K_1
(a) Square nose	1.1
(b) Round nose	1.0
(c) Circular cylinder	1.0
(d) Group of cylinders	1.0
(e) Sharp nose	0.9

K_2 = Correction factor for angle of attack of flow

$$K_2 = \left(\cos\theta + \frac{L}{a}\sin\theta\right)^{0.65}$$

θ = Skew angle of flow with respect to pier, (degrees)

For angles greater than 5°, K_2 dominates; and K_1 should be considered as 1.0.

L = Length of pier (ft, m)

If L/a is larger than 12, use L/a = 12 as a maximum.

V_c = Critical velocity for initiation of erosion of the cohesive material, ft/s (m/s)

$$V_c = K_u\sqrt{\frac{\tau_c H^{1/3}}{\rho g n^2}}$$

$$H = y_1 + y_{s(cont)}$$

The critical velocity can also be determined through material testing (see chapter 4, NCHRP 2004; or Briaud et al. 2011), or it can be estimated for various types of materials using an erosion rate of 0.1 mm/hr in Figure 4.7 of Arneson et al. (2012).

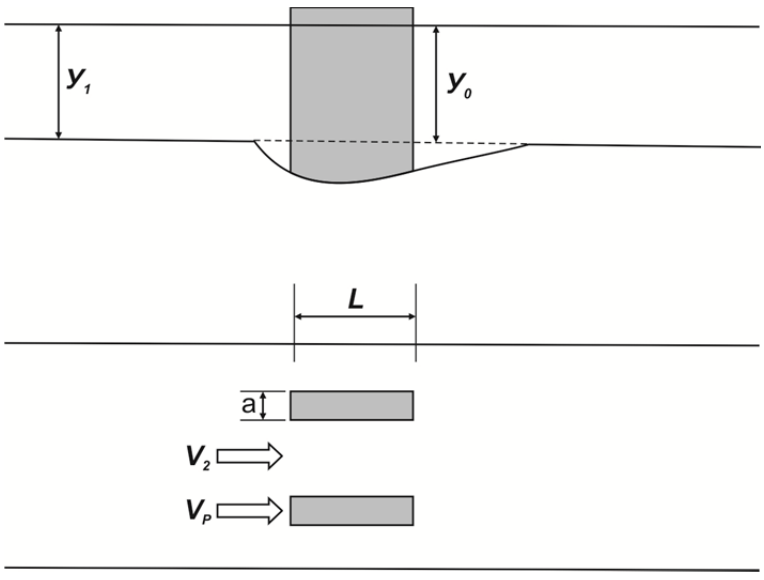

Figure 4. Schematic of parameters used in the cohesive pier and contraction scour method.

Example Problem 1

Given:

Pier geometry: a = 2.5 ft, circular (K_1 and K_2 = 1.0)

Flow variables: y_0 = 11.02 ft, $y_{s(cont)}$ = 2.78 ft, V_p = 5.57 ft/s, n = 0.035

Bed material: τ_c = 0.406 psf

Determine:

The magnitude of the pier scour.

Solution:

1. Compute critical velocity (V_c)

$$H = y_1 + y_{s(cont)} = 11.02 + 2.78 = 13.80 \text{ ft}$$

$$V_c = K_u \sqrt{\frac{\tau_c H^{1/3}}{\rho g n^2}} = 1.486 \sqrt{\frac{0.406 \times 13.80^{1/3}}{1.938 \times 32.2 \times 0.035^2}} = 5.30 \text{ ft/s}$$

2. Compute pier scour ($y_{s(pier)}$)

$$y_{s(pier)} = 2.2 K_1 K_2 a^{0.65} \left(\frac{2.6 V_p - V_c}{\sqrt{g}}\right)^{0.7}$$

$$= 2.2 \times 1.0 \times 1.0 \times 2.50^{0.65} \left(\frac{2.6 \times 5.57 - 5.30}{\sqrt{32.2}}\right)^{0.7} = 5.59 \text{ ft}$$

Example Problem 2

Given:

Pier geometry: a = 5.00 ft, circular (K_1 and K_2 = 1.0)

Flow variables: y_1 = 22.6 ft, $y_{s(cont)}$ = 0, V_p = 3.93 ft/s, n = 0.045

Bed material: τ_c = 0.384 psf

Determine:

The magnitude of the pier scour.

Solution:

1. Compute critical velocity (V_c)

$$H = y_1 + y_{s(cont)} = 22.6 + 0 = 22.6 \text{ ft}$$

$$V_c = K_u \sqrt{\frac{\tau_c H^{1/3}}{\rho g n^2}} = 1.486 \sqrt{\frac{0.384 \times 22.6^{1/3}}{1.94 \times 32.2 \times 0.045}} = 4.35 \text{ ft/s}$$

2. Compute pier scour ($y_{s(pier)}$)

$$y_{s(pier)} = 2.2 K_1 K_2 a^{0.65} \left(\frac{2.6V_p - V_c}{\sqrt{g}}\right)^{0.7}$$

$$= 2.2 \times 1.0 \times 1.0 \times 5.00^{0.65} \left(\frac{2.6 \times 3.93 - 4.35}{\sqrt{32.2}}\right)^{0.7} = 6.41 \text{ ft}$$

4.3 NON-COHESIVE PIER AND CONTRACTION SCOUR MODELING

Hydraulic Engineering Circular No. 18 (HEC-18) (Arneson et al. 2012) scour prediction methods for non-cohesive soils were used to predict scour at each site. These methods were computed in the implementation of selected HEC-18 methods in HEC-RAS. The equations used in HEC-18 are not repeated in this text. Live-bed contraction scour (as indicated by results of equation 6.1 in the HEC-18 manual) was computed at all sites, which means that equations 6.2 and 6.3 in the HEC-18 manual were applied for contraction scour. To be consistent with IDOT general practices, equation 7.1 in the HEC-18 manual (based on the Colorado State University [CSU] equation) was used to calculate pier scour. This equation does not include a K_4 coefficient (correction for armoring by bed material size) as does the original CSU equation, but the K_4 coefficient was generally assumed to be 1 as a conservative measure. Also, IDOT calculates pressure-flow scour; but it was not applied in this study, as the pressure-flow scour would most likely also be applied, in practice, to the results of the ultimate cohesive methods. In other words, only the components of non-cohesive method that can be directly compared with ultimate cohesive method were computed. Abutment scour was not considered in either of the scour methods.

4.4 IDOT COHESIVE SOIL REDUCTION-FACTOR METHOD

Given non-cohesive pier and contraction scour estimates obtained using methods described in the section above, IDOT has determined reduction factors based on unconfined compressive strength (Illinois Department of Transportation 2009). The scour estimates are reduced by the percentage presented in Table 5 for the corresponding unconfined compressive strength ranges.

Table 5. IDOT Cohesive Soil Reduction Factors for Ranges of Unconfined Compressive Strength (Q_u) [ft^2, feet squared].

Q_u (tons/ft^2)	Percent Reduction in Scour Depth
>1.5	50
0.5 – 1.5	25
< 0.5	0

4.5 SCOUR PREDICTION COMPARISONS

Each soil type present at an individual bridge was modeled using the ultimate cohesive scour prediction methods as a hypothetical situation to compare with the non-cohesive scour prediction methods. Analysis at some bridges included multiple soil types because of the variation in the unconfined compressive strength in the soil layers near the potential scour zone. This was a preferred method over averaging the strength parameter, and also showed the variability in scour per soil type. The presence or absence of granular layers was not taken into consideration for the comparison purposes of this study, but obviously would need consideration in an operational application. The comparison of observed scour and the ultimate cohesive, non-cohesive, and reduction-factor 100-year scour predictions methods for each bridge site and soil are presented in Figure 5 and 6 and Table 6.

On average, the application of the non-cohesive method results in the largest predicted scour values, followed by the reduction-factor method results; the ultimate cohesive method application results in the smallest predicted scour value (Table 6). Despite the uncertainties in the field determination of scour (as discussed in section 4.1 Measured Historic Scour), the predicted scour in Figure 6 shows that the ultimate cohesive, non-cohesive, and reduction-factor 100-year scour predictions methods for each bridge site and soil are always higher than observed scour in this study, with the exception of the six predicted values that are all within 0.4 ft of the observed scour.

The ultimate cohesive scour prediction gives a reasonable upper limit to scour, as all the estimates are near or below the non-cohesive method estimates (Figure 5A and 6; Table 6). The ultimate cohesive scour prediction is less than the non-cohesive scour prediction for 78% (38 out of 49) of bridge sites and soils. Seventy-six percent of the ultimate cohesive predictions show a 45% or greater reduction in the non-cohesive predictions over 10 ft. Comparing the ultimate cohesive and reduction-factor 100-year scour predictions methods for each bridge site and soil (Figure 5B and Figure 6; Table 6), the ultimate cohesive scour prediction is less than the reduction-factor scour prediction for 51% (25 out of 49) of bridge sites and soils.

Ultimate cohesive predicted scour is still greater than observed scour when using the confidence intervals for Q_u presented in Table 3 (Figure 7A), with the exception of the six predicted values that are now all within 0.6 ft of the observed scour. Considering the same confidence intervals for Q_u, variability in scour prediction decreases as Q_u increases (Figure 7B and Appendix D).

To further illustrate the sensitivity of scour prediction with varying Q_u, contraction, pier, and total scour are plotted for a range of unconfined compressive strength (Q_u) values (0.5 to 10 tons/ft^2) at bridge sites 3-13 and 5-31 in Figure 8. The 3-13 bridge site gives an example where total scour only varies approximately 2 ft with Q_u varying from 0.5 to 10 tons/ft^2. Also, contraction scour is greater than zero for the full range of Q_u, unlike the example from bridge site 5-13, where contraction scour is predicted to be zero with Q_u values greater than 3 tons/ft^2. These examples show how the ultimate pier and contraction scour in cohesive soils method may be put into practice. Below are three possible steps after the needed hydraulic parameters are obtained for a bridge.

1. Determine the scour for a range of Q_u (0.5 to 10 tons/ft^2).
2. Determine the range of Q_u values for each soil layer in the potential scour zone.
3. Using information from items 1 and 2, decide on a final scour estimate for design.

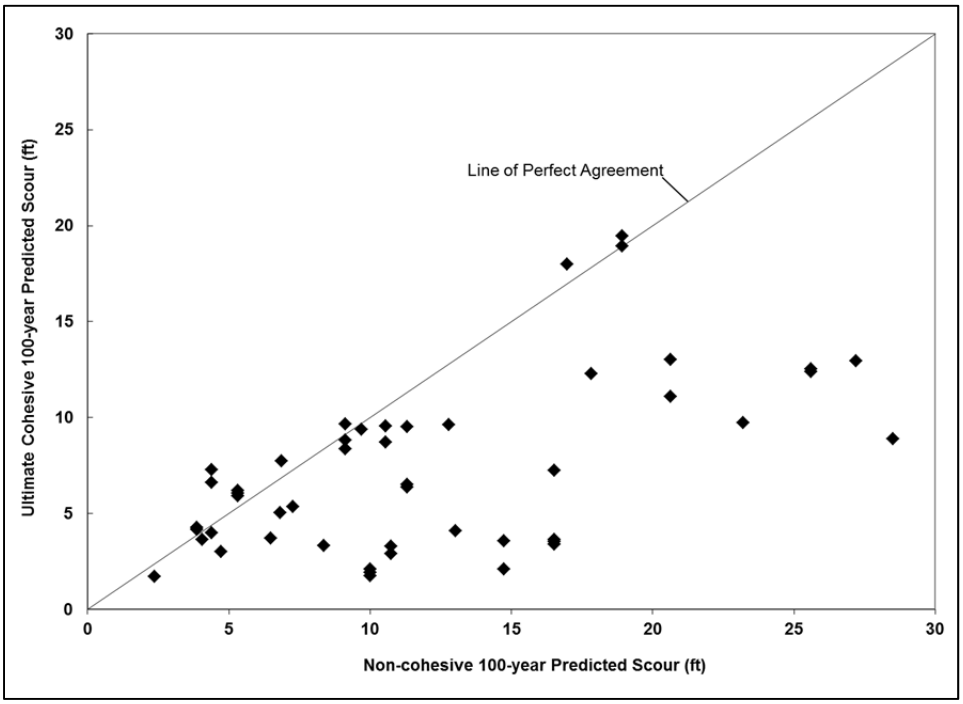

(A)

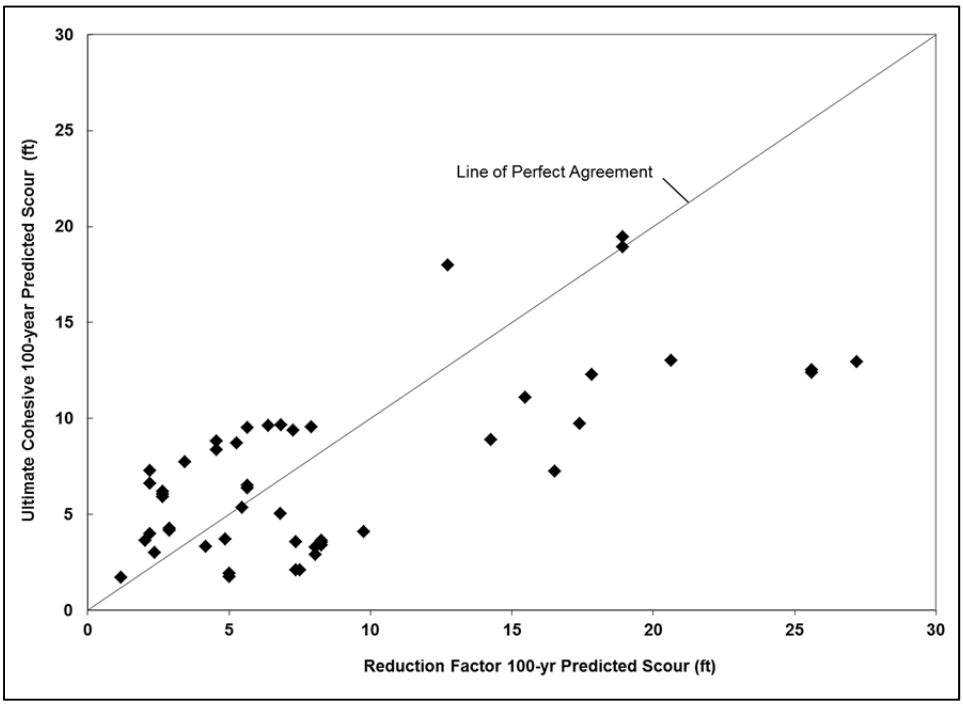

(B)

Figure 5. Ultimate cohesive and non-cohesive (A), and ultimate cohesive and reduction-factor (B) 100-year predicted scours for each bridge site and soil.

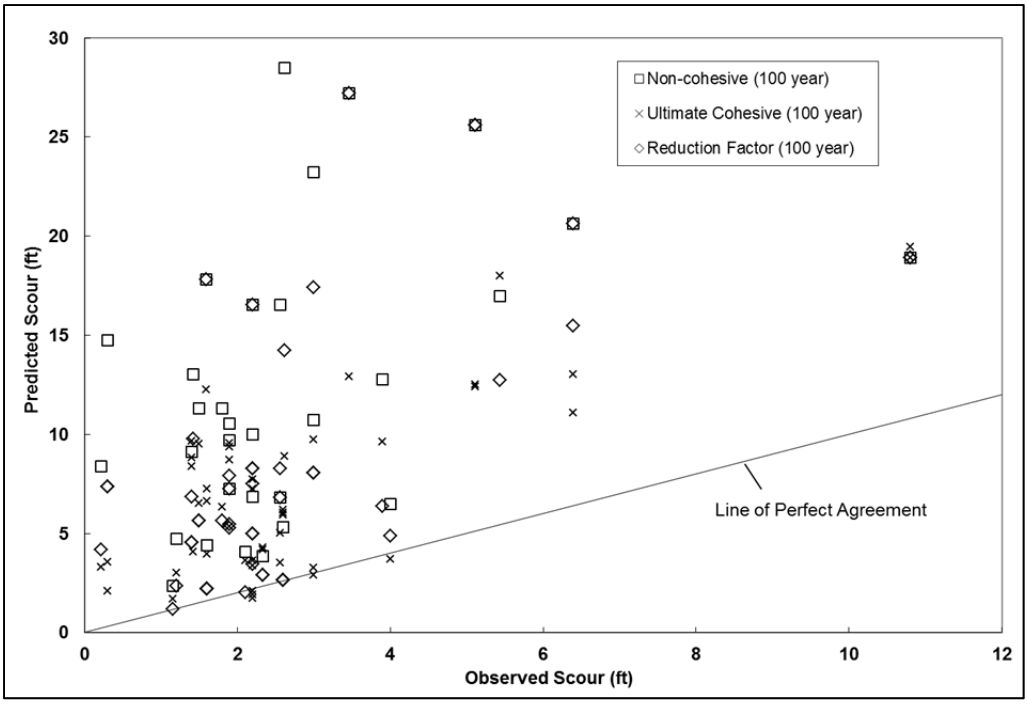

Figure 6. Observed and predicted scour for each bridge site and soil for the 100-year flow, using three scour prediction methods: non-cohesive, ultimate cohesive, and reduction factor.

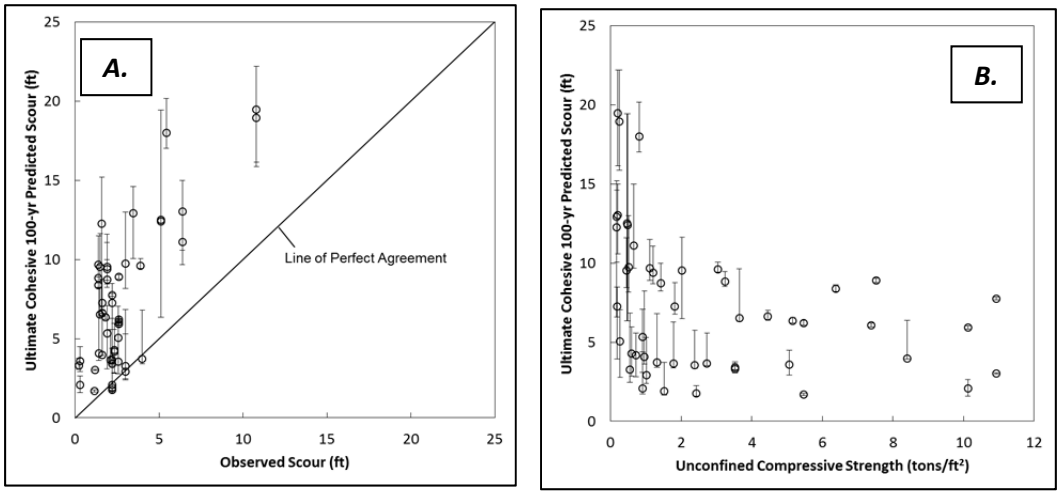

Figure 7. Observed and predicted scour (A), unconfined compressive strength (Q_u), and predicted scour (B) for each bridge site and soil for the 100-year flow, using the ultimate cohesive scour prediction method and including the upper and lower limit of scour prediction, when using the confidence intervals for Q_u presented in Table 3.

Table 6. Unconfined Compressive Strength and Corresponding Observed and Predicted Scour for Each Bridge Site and Soil for the 100-Year and 500-Year Flow, Using Three Scour Prediction Methods: Non-Cohesive, Ultimate Cohesive, and Reduction Factor

[Q_u, unconfined compressive strength; ft, feet; ft^2, feet squared]

Sample	Q_u (tons/ft^2)	Pier and Contraction Scour (ft)					Observed Scour (ft)
		Non-cohesive		Ultimate Cohesive		Reduction	
		100 year	500 year	100 year	500 year	Factor 100 year	
1-1 Soil 1	0.27	6.81	8.10	5.04	5.43	6.81	2.6
1-4 Soil 1	2.39	16.52	17.83	3.54	3.88	8.26	2.6
1-4 Soil 2	0.19	16.52	17.83	7.24	7.92	16.52	2.2
1-4 Soil 3	3.52	16.52	17.83	3.40	3.74	8.26	2.2
1-4 Soil 4	1.78	16.52	17.83	3.65	3.99	8.26	2.2
1-5 Soil 1	1.4	6.49	7.61	3.71	5.71	4.87	4.0
1-6 Soil 1	0.18	17.83	20.31	12.27	12.91	17.83	1.6
1-7 Soil 1	0.72	3.86	4.07	4.17	4.77	2.90	2.3
1-7 Soil 2	0.60	3.86	4.07	4.28	4.87	2.90	2.3
1-8 Soil 1	5.1	14.73	19.84	3.57	7.79	7.37	0.3
1-8 Soil 2	10.1	14.73	19.84	2.09	6.77	7.37	0.3
3-13 Soil 1	6.4	9.12	11.15	8.37	10.54	4.56	1.4
3-13 Soil 2	3.3	9.12	11.15	8.83	11.02	4.56	1.4
3-13 Soil 3	1.2	9.12	11.15	9.67	11.88	6.84	1.4
3-15 Soil 1	1.0	7.27	7.68	5.34	5.90	5.45	1.9
3-25 Soil 1	1.20	9.69	10.42	9.38	10.67	7.27	1.9
3-34 Soil 1	2.8	4.06	4.28	3.65	3.99	2.03	2.1
4-5 Soil 1	0.21	20.63	22.54	13.03	13.65	20.63	6.4
4-5 Soil 2	0.66	20.63	22.54	11.10	11.59	15.47	6.4
5-3 Soil 1	1.9	4.40	4.67	7.26	8.21	2.20	1.6
5-3 Soil 2	4.5	4.40	4.67	6.62	7.53	2.20	1.6
5-3 Soil 3	8.4	4.40	4.67	3.97	7.10	2.20	1.6
5-17 Soil 1	5.47	2.37	3.82	1.70	1.82	1.19	1.2
5-20 Soil 1	3.53	8.37	9.77	3.31	3.71	4.19	0.2
5-21 Soil 1	5.2	11.30	12.64	6.36	10.65	5.65	1.8
5-24 Soil 1	5.5	5.31	7.19	6.19	6.90	2.66	2.6
5-24 Soil 2	7.4	5.31	7.19	6.06	6.76	2.66	2.6
5-24 Soil 3	10.1	5.31	7.19	5.92	6.61	2.66	2.6
5-25 Soil 1	1.6	10.01	10.07	1.91	2.28	5.01	2.2
5-25 Soil 2	1.0	10.01	10.07	2.09	2.45	7.51	2.2
5-25 Soil 3	2.5	10.01	10.07	1.75	2.14	5.01	2.2
5-26 Soil 1	10.9	4.72	5.49	3.02	3.50	2.36	1.2
5-27 Soil 1	10.9	6.87	8.13	7.75	9.27	3.44	2.2
5-31 Soil 1	2.1	11.30	12.64	9.53	11.61	5.65	1.5
5-31 Soil 2	3.7	11.30	12.64	6.52	10.99	5.65	1.5
6-22 Soil 1	0.97	13.02	17.96	4.07	3.97	9.77	1.4
7-1 Soil 1	0.21	18.93	13.25	19.47	21.30	18.93	10.8
7-1 Soil 2	0.25	18.93	13.25	18.93	20.72	18.93	10.8
7-18 Soil 1	7.53	28.50	25.06	8.89	8.36	14.25	2.6
7-31 Soil 1	3.1	12.78	13.01	9.61	3.50	6.39	3.9
7-32 Soil 1	0.6	10.73	12.64	3.28	11.12	8.05	3.0
7-32 Soil 2	1.1	10.73	12.64	2.91	10.65	8.05	3.0
8-3 Soil 1	0.81	16.97	17.09	17.99	18.60	12.73	5.4
8-50 Soil 1	0.51	23.21	18.02	9.74	2.79	17.41	3.0
8-82 Soil 1	0.5	10.54	11.86	9.55	11.28	7.91	1.9
8-82 Soil 2	1.5	10.54	11.86	8.71	10.41	5.27	1.9
9-1 Soil 1	0.18	27.20	22.05	12.94	13.48	27.20	3.5
9-2 Soil 1	0.47	25.60	28.00	12.52	14.60	25.60	5.1
9-2 Soil 2	0.49	25.60	28.00	12.40	14.48	25.60	5.1
Average		12.10	12.89	7.21	8.44	8.66	2.8

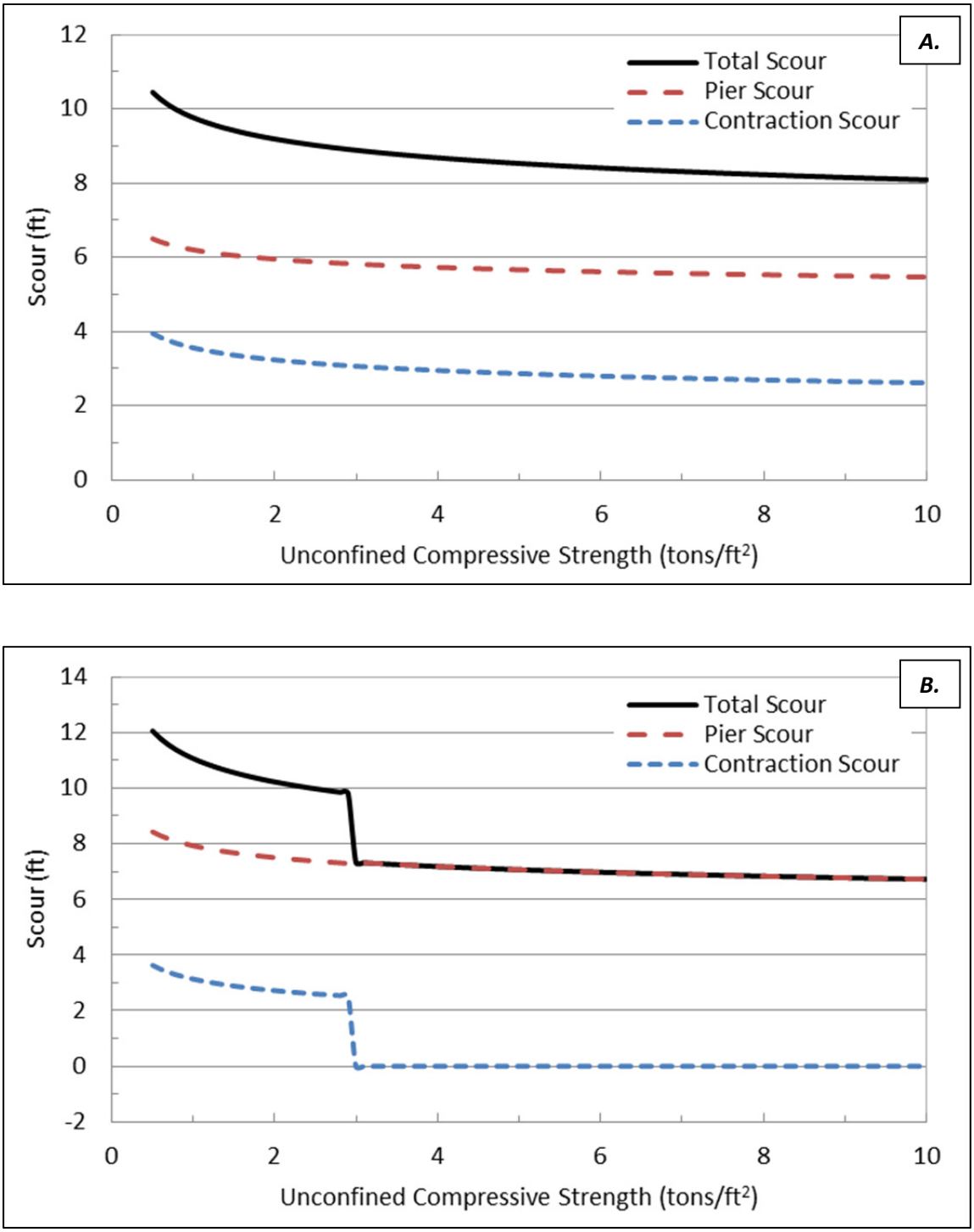

Figure 8. Contraction, pier, and total scour, for a range of unconfined compressive strength (Q_u) values (0.5 to 10 tons/ft^2) at bridge sites 3-13 (A) and 5-31 (B).

CHAPTER 5 SUMMARY AND CONCLUSIONS

The SRICOS-EFA methodology outlined in National Cooperative Highway Research Program (NCHRP) Report 516 (2004) was tested in Illinois at 15 sites (Straub and Over 2010). The method was updated in Briaud et al. (2011), and the update was also included in the Federal Highway Administration Hydraulic Engineering Circular No. 18 (HEC-18) (Arneson, et al. 2012). The Straub and Over (2010) study showed that the IDOT cohesive soil reduction-factor method (adjusting the FHWA's non-cohesive estimates using the soil unconfined compressive strength) may not, by itself, always provide the best estimate of bridge scour, and that computing SRICOS ultimate scour—previously called Zmax—(using the soil unconfined compressive strength and hydraulic properties) may improve the estimate of scour. The SRICOS ultimate scour is the equilibrium maximum contraction and pier scour of cohesive soils over time. To further test the SRICOS ultimate scour method in Illinois, the U.S. Geological Survey (USGS), in cooperation with the Illinois Center for Transportation and the Illinois Department of Transportation (IDOT), began a study in 2011 at 15 additional bridge sites throughout the state.

The purpose of this report is to present a comparison of the ultimate cohesive and non-cohesive methods, along with the reduction-factor method and observed scour. The combined results of the 15 bridge sites in the original study and the 15 additional bridge sites in this study are presented. Also, results of the comparison of historic IDOT laboratory and field values of unconfined compressive strength are presented. The unconfined compressive strength is used in both ultimate cohesive and the reduction-factor methods, thus knowing how the field-determined values compare to the laboratory-determined values is critical to the reliability of the application of both methods.

On average, the non-cohesive method results predict the highest amount of scour, followed by the reduction-factor method results, and the ultimate cohesive method results predict the lowest amount of scour. The predicted scour for the ultimate cohesive, non-cohesive, and reduction-factor 100-year scour predictions methods for each bridge site and soil are always higher than observed scour in this study, with the exception of the 12% of predicted values that are all within 0.4 ft of the observed scour. The ultimate cohesive scour prediction method is less than the non-cohesive scour prediction method for 78% of bridge sites and soils. At the sites where this occurs, the soil types reflect a wide range of Q_u values (0.21 to 10.9 tons/ft^2), so a combination of Q_u, hydraulic and bridge parameters all play a role in the ultimate cohesive scour prediction.

Seventy-six percent of the ultimate cohesive predictions show a 45% or greater reduction in the non-cohesive predictions that are over 10 ft. When the ultimate cohesive and reduction-factor 100-year scour predictions methods are compared for each bridge site and soil, the ultimate cohesive scour prediction method is less than the reduction-factor 100-yr scour prediction method for 51% of bridge sites and soils.

Critical shear stress remains a needed parameter in the ultimate scour prediction for cohesive soils; and the unconfined soil compressive strength (Q_u), as measured by IDOT in the laboratory, was found in an earlier study (Straub and Over 2010) to provide a good prediction of critical shear stress, as measured by using the erosion function apparatus (EFA). Because laboratory Q_u analyses are time-consuming and expensive, the ability of field-measured Rimac data to estimate unconfined soil strength in the critical shear–soil strength relation was tested. A regression analysis was completed using an historic IDOT dataset containing 366 data pairs of laboratory Q_u and Rimac measurements from common sites with cohesive soils.

The proposed Rimac-Q_u relation is composed of a combination of two equations and their prediction intervals, one coming from a linear fit to the smaller Rimac and Q_u values after log-transformation and the other from a linear fit to the larger Rimac and Q_u values without transformation. The values of these coefficients and their confidence intervals show that at the 5% significance level, the untransformed slope is not significantly different from 1, the untransformed intercept is not significantly different from 0, the log-log slope is not significantly different from 1, and the log-log intercept is not significantly different from 0. These findings mean that neither equation is significantly different from the identity Q_u = Rimac. The alternative predictions of ultimate cohesive scour presented in this study assume Q_u will be estimated using Rimac measurements that include computed uncertainty. In particular, the ultimate cohesive predicted scour is greater than observed scour for the entire 90% confidence interval range for predicting Q_u at the bridges and soils used in this study, with the exception of the six predicted values that are all within 0.6 ft of the observed scour.

The sources of uncertainty in applying the methods of this study include uncertainty of scour measurements, non-homogeneous nature of soils that may introduce error into estimated soil properties, uncertainty of hydraulic models, and uncertainty associated with flow data. To determine whether the methods presented in this report are applicable to a given site for prediction of pier and contraction scour, the range of site characteristics used in this study should be considered.

REFERENCES

Arneson, L.A., L.W. Zevenbergen, P.F. Lagasse, and P.E. Clopper. 2012. *Evaluating Scour at Bridges*. U.S. Department of Transportation, Federal Highway Administration, Washington, D.C. Hydraulic Engineering Circular No. 18, 5th ed., Publication No. FHWA-HIF-12-003. 340 pp.

Benedict, S.T. 2003. *Clear-Water Abutment and Contraction Scour in the Coastal Plain and Piedmont Provinces of South Carolina, 1996–99*. Water-Resources Investigations Report 03-4064, U.S. Geological Survey, Reston, VA, 137 pp.

Brandimarte, L., A. Montanari, J.-L. Briaud, and P. D'Odorico. 2006. "Stochastic flow analysis for predicting scour of cohesive soils." *Journal of Hydraulic Engineering* 132(5):493–500.

Briaud, J.-L., and H.-C. Chen. 2005. "The EFA, erosion function apparatus: An overview." In *Proceedings of the International Conference on Soil Mechanics and Geotechnical Engineering*, Osaka, Japan, September 2005.

Briaud, J.-L., H.-C. Chen, K.-A. Chang, S.J. Oh, S. Chen, J. Wang, Y. Li, K. Kwak, P. Nartjaho, R. Gudaralli, W. Wei, S. Pergu, Y.W. Cao, and F. Ting. 2011. *The SRICOS-EFA Method, Summary Report,* Texas A&M University. https://ceprofs.civil.tamu.edu/briaud/SRICOS-EFA/Summary%20of%20SRICOS-EFA%20Method.pdf (accessed February 2013).

Briaud, J.-L., H.-C. Chen, L.P. Nurtjahyo, and J. Wang. 2004. "The SRICOS-EFA method for complex fine grained soils." *Journal of Geotechnical and Geoenvironmental Engineering* 130(11):1180–1191.

Carroll, R.J., and D. Ruppert. 1996. "The use and misuse of orthogonal regression in linear errors-in-variables models." *The American Statistician* 50(1):1–6.

Curry, J.E., S.H. Crim, Jr., O. Güven, J.G. Melville, and S. Santamaria. 2003. *Scour Evaluations of Two Bridge Sites in Alabama with Cohesive Soils*. Final report for Alabama Department of Transportation Research Project 930-490R.

Dingman, S.L. 1994. *Physical Hydrology*. Upper Saddle River, New Jersey: Prentice-Hall. 575 pp.

Flaxman, E. M. 1963. "Channel Stability in Undisturbed Cohesive Soils" Journal of the Hydraulic Division, Proceedings of the ASCE, Vol. 89, No. HY2, Proceeding Paper 3462, March 1963, pp. 87-96.

Fuller, W.A. 1987. *Measurement Error Models*. New York: John Wiley and Sons. 440 pp.

Ghelardi, V.M. 2004. *Estimation of Long Term Bridge Scour in Cohesive Soils at Maryland Bridges Using EFA/SRICOS*. Master's Thesis, University of Maryland, College Park, MD. 76 pp.

Helsel, D.R., and R.M. Hirsch. 2002. "Statistical Methods in Water Resources." *Techniques of Water-Resources Investigations of the United States Geological Survey,* Book 4, Chapter A3. Reston, VA: U.S. Geological Survey. 510 pp.

Hirsch, R.M. 1982. "A comparison of streamflow record extension techniques." *Water Resources Research* 18(4):1081–1088.

Hirsch, R.M., and E.J. Gilroy. 1984. "Methods of fitting a straight line to data: Examples in water resources." *Water Resources Bulletin* 20(5):705–710.

Illinois Department of Transportation (IDOT). 2009. *Bridge Manual*. Bureau of Bridges and Structures, Springfield, IL. 834 pp. http://www.dot.state.il.us/bridges/brmanuals.html (accessed February 2013).

Ivarson, W.R. 1998, “Scour and Erosion in Clay Soils”, ASCE Compendium of Conference Scour Papers (1991 to 1998), pp. 280-287, Reston, VA.

National Cooperative Highway Research Program, 2004, “Pier and Contraction Scour in Cohesive Soils,” NCHRP Report 516, Transportation Research Board, National Academy of Science, Washington, D.C. (Briaud, J.L., H.-C. Chen, Y. Li, P. Nurtjahyo, and J. Wang).

Soong, D.T., A.L. Ishii, J.B. Sharpe, and C.F. Avery. 2004. *Estimating Flood-Peak Discharge Magnitudes and Frequencies for Rural Streams in Illinois*. U.S. Geological Survey Scientific Investigations Report 2004-5103. 147 pp.

Straub, T.D., and T.M. Over. 2010. *Pier and Contraction Scour Prediction in Cohesive Soils at Selected Bridges in Illinois*. Illinois Center for Transportation, Research Report ICT-10-074. Rantoul, IL. 133 pp.

Sturm, T., F. Sotiropoulos, M. Landers, T. Gotvald, S. Lee, L. Ge, R. Navarro, and C. Escauriaza. 2004. *Laboratory and 3D Numerical Modeling with Field Monitoring of Regional Bridge Scour in Georgia*. Final report for Georgia Department of Transportation Research Project No. 2002, Atlanta, GA.

Ting, F.C.K., A.L. Jones, and R.J. Larsen. 2010. *Evaluation of SRICOS Method on Cohesive Soils in South Dakota*. Department of Civil and Environmental Engineering, South Dakota State University, Brookings, SD. 235 pp.

U.S. Army Corps of Engineers. 2010. *River Analysis System Reference Manual* (version 4.1.0). Hydraulic Engineering Center, Davis, CA.

Warton, D.I., R.A. Duursma, D.S. Falster, and S. Taskinen. 2012. “smatr 3—An R package for estimation and inference about allometric lines.” *Methods in Ecology and Evolution* 3(2):257259.

APPENDIX A IDOT HISTORIC UNCONFINED COMPRESSIVE STRENGTH AND RIMAC DATA

Four scatterplots of Rimac versus Q_u values from a dataset containing 366 data pairs were obtained from IDOT. Basic statistics were attached to each plot. The original IDOT plots and associated statistical analyses are included below. The second plot, titled "CLAYS," is labeled as including clay and clay loam and contains 92 data points, according to the statistical analysis attached. The third plot, titled "SILTS," is labeled as including "Silt, SiL, SiC, and SiCL" (assumed to designate silt, silt loam, silty clay, and silty clay loam, respectively, by comparison with the standard soil-texture triangle, e.g., Dingman 1994, p. 213) and includes 253 data points. The fourth plot, titled "SANDS," is labeled as including "Sa, SaL, Sac, SaCL, and Loam" (assumed to designate sand, sandy loam, sandy clay, sand clay loam, and loam, respectively) and includes 21 data points. Because of the range of soil textures included in each plot, it is not surprising that the range of soil strengths represented in the plots is also rather wide. The terminology SANDS, SILTS, and CLAYS is retained in this appendix in referring to the plots for convenience; but these titles are not to be taken literally with respect to the soil textures for many of the soil samples included.

The numerical data and textural classification on which these plots were based could not be retrieved. The USGS therefore digitized the data pairs from the plots and obtained a dataset with 325 total paired Q_u and Rimac values, along with a classification into the soil texture (sand, silt, or clay) for each data point. A comparison of the original and digitized datasets is provided in Table A1. It can be seen that most the points from the SANDS and CLAYS plots were able to be digitized, and likewise the regression coefficients are quite similar. Somewhat fewer data were recovered from the SILTS plot, and the regression coefficients are somewhat different; but both the original intercept and slope are within or near the uncertainty band of the coefficient obtained from the digitized data (that is, the coefficient +/- its standard error). The all-data case is similar to the SILTS case. As a result, we conclude that the number of points recovered and the similarity of the regression coefficients indicate that the digitized data provide a representative sample of the original data.

Table A1. Statistical Properties of IDOT's Original Q_u-Rimac Dataset and of the Subset Obtained by USGS from Digitizing Points from the Scatterplots of the Original Dataset
[N, number of points]

Plot title	Original data			Digitized data		
	N	Slope of linear regression of Rimac vs. Q_u ("b coefficient")	Intercept of linear regression of Rimac vs. Q_u ("a coefficient")	N	Slope of linear regression of Rimac vs. Q_u +/- standard error	Intercept of linear regression of Rimac vs. Q_u +/- standard error
"SANDS"	21	0.3620	0.4909	20	0.3571 +/- 0.4021	0.4893 +/- 0.2022
"SILTS"	253	0.4740	0.4726	218	0.4446 +/- 0.0575	0.5319 +/- 0.0694
"CLAYS"	92	0.8116	0.3059	87	0.8262 +/- 0.0777	0.3258 +/- 0.1418
All data	366	0.6995	0.3848	325	0.6557 +/-0.0440	0.3984 +/- 0.0604

There is significant scatter in the plots showing the Rimac and Q_u soil strength estimates. These differences arise from many sources, of which the testing procedure is only one. The paired Q_u and Rimac values come from common sites, but they are from different soil samples obtained using different samplers. Along with the numerical and textural data not being retrieved, the location and timing of each sample could not be retrieved; and it is assumed that at least some of the paired data could have been taken at different locations within the site and possibly at different times. The effect of the different samplers is an inherent difference in the Q_u and Rimac testing methods; however, sampling variability affects the present analysis but would not affect a comparison of Q_u and Rimac measurements of the same soil sample. Therefore, sampling variability is adding an unknown amount of noise to the present comparison of Q_u and Rimac measurements. Although the texture (based on the grain-size distribution) is a fundamental property of soils, in the present context, it is not possible to recover the textural classification of the sample data beyond the three broad groupings described above; nor is it currently routine operation to do grain-size analyses from soil samples at bridge sites. Therefore, the relations between Q_u and Rimac presented here were developed based on the whole dataset.

Qu vs RIMAC

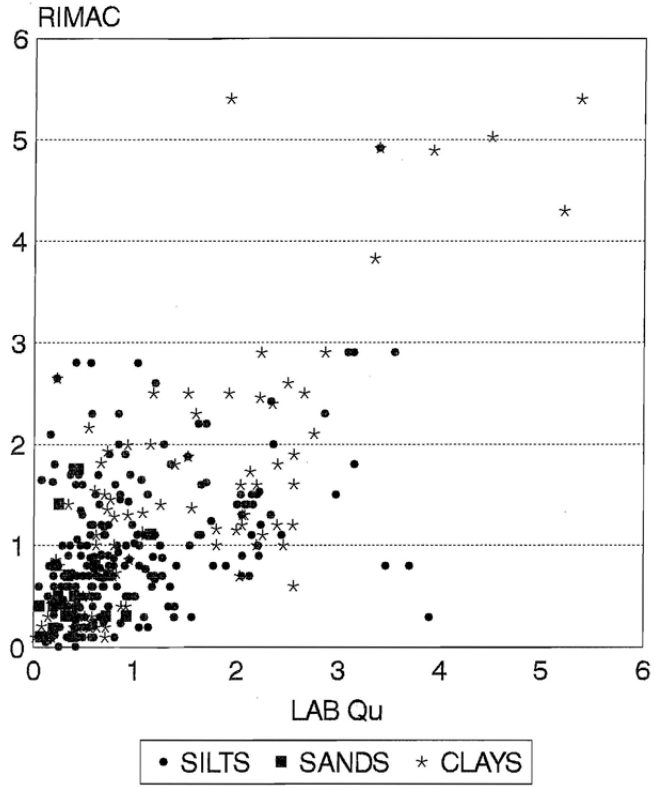

Qu vs RIMAC
SANDS,SILTS,&CLAYS

Total Number of Data Points	366
Minimum Value	0.01
Maximum Value	5.38
Average	1.02249
Median	0.8
Standard Deviation	0.8856
Correlation Coefficient	0.6368
R-Squared	0.4055
Regression Type	Trend
a Coefficient	0.38481
b Coefficient	0.6995

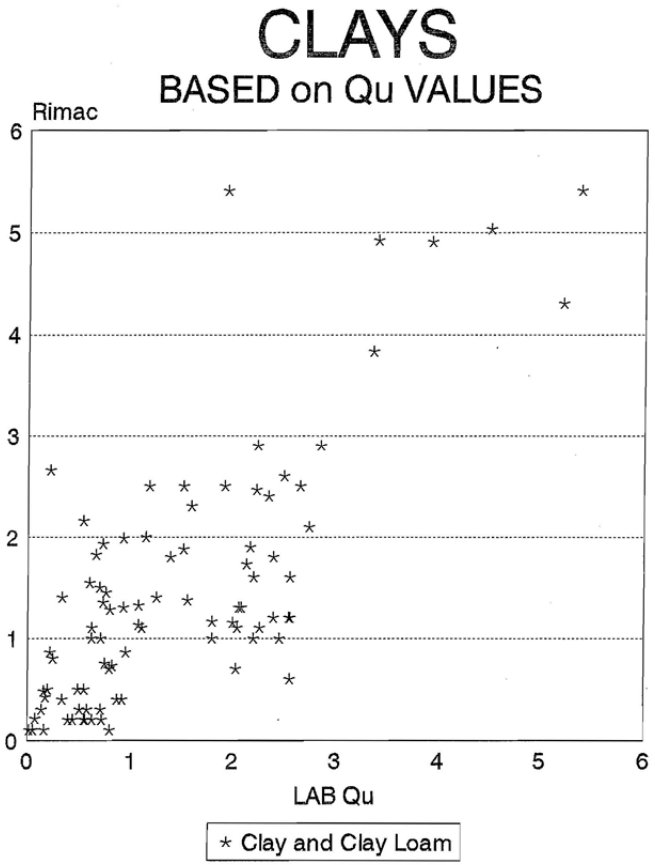

Qu vs RIMAC
CLAY

Total Number of Data Points	92
Minimum Value	0.02
Maximum Value	5.38
Average	1.46108
Median	1.2
Standard Deviation	1.2217
Correlation Coefficient	0.7445
R-Squared	0.5542
Regression Type	Trend
a Coefficient	0.3059
b Coefficient	0.81162

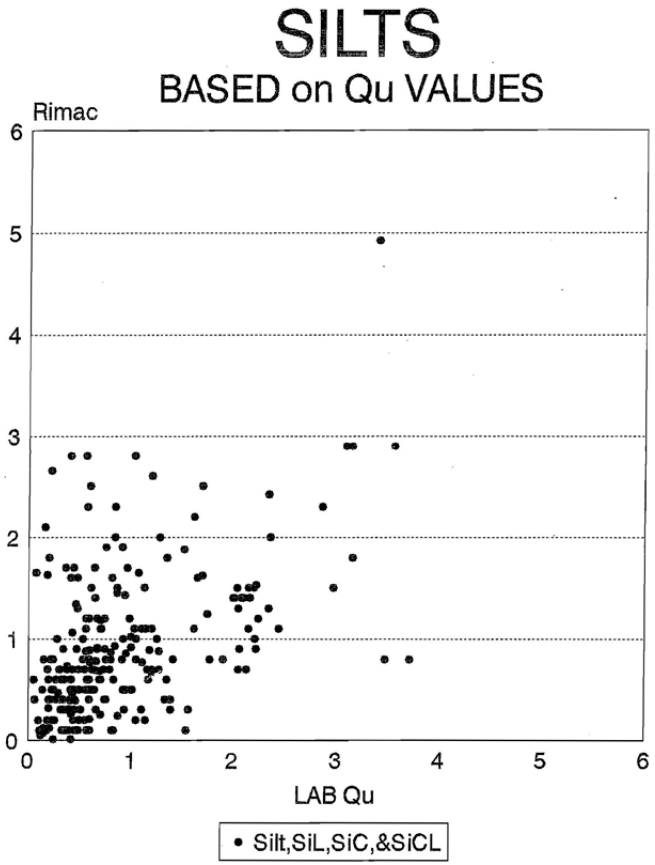

Qu vs RIMAC
SILTS

Total Number of Data Points	253
Minimum Value	0.01
Maximum Value	4.92
Average	0.8903
Median	0.7
Standard Deviation	0.6977
Correlation Coefficient	0.4931
R-Squared	0.2431
Regression Type	Trend
a Coefficient	0.4726
b Coefficient	0.4740

SANDS

BASED on Qu VALUES

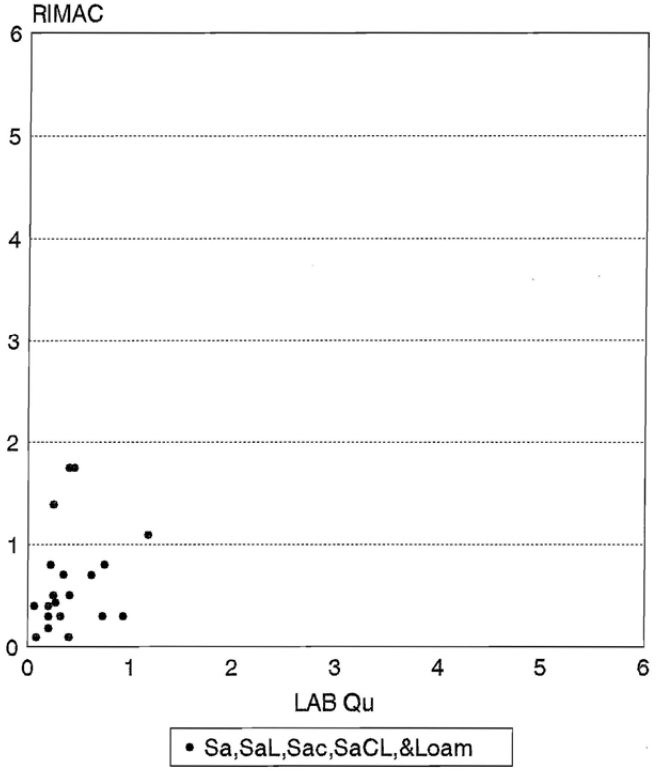

Qu vs RIMAC

SAND

Total Number of Data Points	21
Minimum Value	0.06
Maximum Value	1.75
Average	0.6405
Median	0.465
Standard Deviation	0.4882
Correlation Coefficient	0.2093
R-Squared	0.0438
Regression Type	Trend
a Coefficient	0.4909
b Coefficient	0.3620

APPENDIX B UNCONFINED COMPRESSIVE STRENGTH AND RIMAC REGRESSION DETAILS

For reasons discussed below, a line of organic correlation (LOC) regression technique was chosen here for use in developing the Q_u-Rimac relation. To the best of our knowledge, there is no standard method for computing prediction intervals for LOC regression. In light of this situation, the 90% prediction intervals shown in Figure 3 were computed with the standard ordinary least squares (OLS) prediction interval equation (Helsel and Hirsch 2002, p. 241):

$$\left(y_0 - ts\sqrt{1+\frac{1}{n}+\frac{(x_0-\bar{x})^2}{SS_x}}, y_0 + ts\sqrt{1+\frac{1}{n}+\frac{(x_0-\bar{x})^2}{SS_x}} \right),$$

where y_0 is the predicted y (Q_u) value when the Rimac value is x_0, t is the value of the Student's *t* distribution having $n-2$ degrees of freedom with an exceedance probability of 0.05, s is the standard error of regression, n is the number of data points used in the regression, $\bar{x}$ is the mean of the *x* (Rimac) values, and $SS_x = \sum_{i=1}^{n}(x_i - \bar{x})^2$ is the *x* (Rimac) sum of squares. Values of all these quantities are given in Table 3, except for the value of the *t* distribution, which is a standard statistical distribution tabulated in statistical tables. As there are two prediction intervals shown in Figure 3, one each from the log-log and non-transformed regressions, the applicable lines to use for the prediction interval for a given Rimac value are the ones closer to the center, even if that means the prediction interval line from the log-log regression is used for one line and the non-transformed line is used for the other, as would be the case for Rimac near 1. As can be seen in Figure 3, the prediction intervals create an approximate envelope curve around the scatter of the data, with 7 of 130 red points and 19 of 195 black points lying outside, for a total of 26 of 325 or 8% lying outside. This percentage approximately matches the 10% that corresponds to the chosen 90% prediction interval, which corroborates the reasonableness of the method of computing them.

As mentioned, the linear fits presented here were computed using a regression procedure called the line of organic correlation (LOC), as implemented in the function *sma* from the *R* package *smatr* (Warton et al. 2012), where it is called the standardized major axis (SMA). The differences between the LOC and the most commonly used regression procedure, OLS, can be characterized in several ways. From a computational perspective, whereas OLS minimizes the sum of squared deviations of the y-axis values from the fitted line, the LOC minimizes the "sum of the areas of right triangles formed by horizontal and vertical lines extending from observations to the fitted line" (Helsel and Hirsch 2002, p. 277). The LOC slope also can be computed as the geometric mean of the slopes obtained by OLS regression of y on x and x on y. Both of these descriptions of the means of computing the LOC slope show that LOC takes into account errors in both variables and indeed treats both variables equivalently.

The LOC solution arises as the optimal linear fit when both the x- and y-variables have measurement and/or sampling errors (sometimes called an errors-in-variables model, Carroll and Ruppert 1996) under conditions that are symmetric in x and y in the following

sense: when the ratio of the error variances (x-error over y-error) is equal to the ratio of the x-data variance to the y-data variance (Hirsch and Gilroy 1984). Although the errors in the Rimac and Q_u data are unknown, the variance of the Rimac data are 0.8494, and the variance of the Q_u data are 0.8048; so their ratio is near one. If the Q_u measurement/ sampling error plus the equation error (which is the error arising from the failure of the linear model to be exactly correct) is similar to the Rimac measurement error, then the error variance ratio would also be near one. Thus the interpretation of the LOC solution of the Q_u versus Rimac relation as error-in-variables model seems plausible. The effect of the errors in the x-variable on the regression (if OLS regression were used) is to attenuate (that is, reduce the absolute value of) the slope estimate (Fuller 1987, chapter 1). In the present case, the OLS slope estimate for the log-transformed data with Rimac < 1.06 is 0.2214 and for the non-transformed data with Rimac > 1.06 it is 0.3953. As predicted, both are significantly smaller than the LOC slope estimates presented in Table 3.

Another difference between OLS and LOC fits is that predictions from the x-data using the OLS line reproduce the mean of the y-data and minimize the squared error of individual predictions with the result of underpredicting the variance of the y-data, whereas predictions from the x-data using the LOC line reproduce both the mean and the variance of the y-data. For this reason, LOC is often used to compute a relationship for use in extending hydrologic records (Helsel and Hirsch 2002, p. 277) by the so-called maintenance-of-variance-extension (MOVE) procedure (Hirsch 1982). The loss of variance in the predicted y-values in the case of the OLS fit would mean an underprediction of large values of Q_u and an overprediction of small values of Q_u for a given value of Rimac. From a practical point of view, this situation of attenuation of the predicted range of Q_u values was the primary reason for selecting the LOC approach to constructing the Q_u-Rimac relation presented here.

APPENDIX C VALUES FOR VARIABLES USED IN SCOUR PREDICTION

Values for variables used in 100-yr flow scour prediction [tsf, tons per square foot]

	Parameters for ultimate cohesive scour prediction										Additional parameters for non-cohesive scour prediction						
Bridge site and soil	Pier shape	Angle of attack (degrees)	Pier length L (ft)	Pier width a (ft)	Existing bridge contraction channel average depth y_0 (ft)	Approach channel average depth y_1 (ft)	Contracted channel average velocity[1] V_2 (ft/s)	Velocity upstream of pier[2] V_p (ft/s)	Manning's n	Q_u (tsf)	Approach channel average velocity[1] (ft/s)	Channel flow through the bridge opening (ft^3/s)	Channel top width inside the bridge opening (ft)	Channel flow through the approach section (ft^3/s)	Channel top width at the approach cross section (ft)	Median diameter of bed material[3] D_{50} (mm)	Flow depth directly upstream of pier (ft)
1-1 Soil 1	Round	0	130.0	3.50	13.19	11.30	2.13	2.13	0.045	0.27	1.70	6863	232	6429	335	0.0041	13.26
1-4 Soil 1	Round	0	49.8	3.00	14.23	11.68	2.90	2.90	0.045	2.39	1.75	6368	142	5940	290	0.0148	14.66
1-4 Soil 2	Round	0	49.8	3.00	14.23	11.68	2.90	2.90	0.045	0.19	1.75	6368	142	5940	290	0.0100	14.66
1-4 Soil 3	Round	0	49.8	3.00	14.23	11.68	2.90	2.90	0.045	3.52	1.75	6368	142	5940	290	0.0217	14.66
1-4 Soil 4	Round	0	49.8	3.00	14.23	11.68	2.90	2.90	0.045	1.78	1.75	6368	142	5940	290	0.0149	14.66
1-5 Soil 1	Round	0	80.0	2.50	14.36	12.24	3.18	3.18	0.045	1.40	3.11	3232	55.5	3232	85	0.03	13.69
1-6 Soil 1	Round	0	61.8	21.20	13.57	12.28	1.69	1.69	0.045	0.18	1.72	6385	177	6313	299	0.0084	14.41
1-7 Soil 1	Square	0	109.8	2.44	10.40	8.14	2.08	2.08	0.065	0.72	2.69	2180	96	2172	99	0.1296	10.46
1-7 Soil 2	Square	0	109.8	2.44	10.40	8.14	2.08	2.08	0.065	0.60	2.69	2180	96	2172	99	0.0679	10.46
1-8 Soil 1	Round	0	63.4	20.00	11.21	14.85	1.89	1.89	0.043	5.10	2.29	3355	130	3608	106	0.03	14.87
1-8 Soil 2	Round	0	63.4	20.00	11.21	14.85	1.89	1.89	0.043	10.10	2.29	3355	130	3608	106	0.03	14.87
3-13 Soil 1	Round	0	46.0	2.50	11.02	10.80	5.57	5.57	0.035	6.40	4.55	7121	100	5303	108	0.03	11.03
3-13 Soil 2	Round	0	46.0	2.50	11.02	10.80	5.57	5.57	0.035	3.30	4.55	7121	100	5303	108	0.03	11.03
3-13 Soil 3	Round	0	46.0	2.50	11.02	10.80	5.57	5.57	0.035	1.20	4.55	7121	100	5303	108	0.03	11.03
3-15 Soil 1	Round	0	18.0	2.00	8.82	13.55	3.29	3.29	0.045	1.00	2.54	3363	123	2511	73	0.03	15.45
3-25 Soil 1	Round	0	46.0	2.50	11.15	9.70	5.52	5.52	0.035	1.20	6.5	5366	83	5670	90	0.0591	11.31
3-34 Soil 1	Round	0	27.0	2.00	8.50	5.52	3.96	3.96	0.035	2.80	6.2	5460	126	5460	159	0.03	10.51
4-5 Soil 1	Round	0	42.0	3.99	29.51	22.58	4.34	4.34	0.045	0.21	5.21	38292	147	23234	198	0.0148	29.30
4-5 Soil 2	Round	0	42.0	3.99	29.51	22.58	4.34	4.34	0.045	0.66	5.21	38292	147	23234	198	0.0204	29.30
5-3 Soil 1	Round	0	30.0	2.00	11.89	14.86	4.58	4.58	0.040	1.90	6.29	5256	92	5155	55	0.03	11.92
5-3 Soil 2	Round	0	30.0	2.00	11.89	14.86	4.58	4.58	0.040	4.50	6.29	5256	92	5155	55	0.03	11.92
5-3 Soil 3	Round	0	30.0	2.00	11.89	14.86	4.58	4.58	0.040	8.40	6.29	5256	92	5155	55	0.03	11.92
5-17 soil 1	Round	0	29.8	1.00	9.66	8.69	3.38	3.38	0.035	5.47	3.24	4080	125	4078	145	0.0213	9.12
5-20 Soil 1	Round	0	38.0	4.50	11.50	12.07	2.58	2.58	0.040	3.53	2.38	3887	108	4202	147	0.0274	13.89
5-21 Soil 1	Round	0	130.0	5.00	20.06	22.59	3.93	3.93	0.045	5.20	3.57	15703	200	11690	145	0.03	22.14
5-24 Soil 1	Round	0	46.0	1.33	7.99	8.79	5.19	5.19	0.039	5.50	3.58	1600	50.2	723	23	0.03	5.05
5-24 Soil 2	Round	0	46.0	1.33	7.99	8.79	5.19	5.19	0.039	7.40	3.58	1600	50.2	723	23	0.03	5.05
5-24 Soil 3	Round	0	46.0	1.33	7.99	8.79	5.19	5.19	0.039	10.10	3.58	1600	50.2	723	23	0.03	5.05
5-25 Soil 1	Round	0	33.0	1.75	6.43	8.87	2.38	2.38	0.040	1.60	2.87	3029	80.5	1223	48	0.03	9.08
5-25 Soil 2	Round	0	33.0	1.75	6.43	8.87	2.38	2.38	0.040	1.00	2.87	3029	80.5	1223	48	0.03	9.08
5-25 Soil 3	Round	0	33.0	1.75	6.43	8.87	2.38	2.38	0.040	2.50	2.87	3029	80.5	1223	48	0.03	9.08
5-26 Soil 1[A]	Round	0	47.5	2.45	8.33	6.49	2.86	2.86	0.050	10.90	2.06	2571	96.8	6693	501	0.03	13.42
5-27 Soil 1	Round	0	47.5	2.45	10.94	8.91	4.77	4.77	0.050	10.90	3.26	13629	312	9507	327	0.03	15.24
5-31 Soil 1	Round	0	130.0	5.00	20.06	22.59	3.93	3.93	0.045	2.10	3.57	15703	200	11690	145	0.03	22.14
5-31 Soil 2	Round	0	130.0	5.00	20.06	22.59	3.93	3.93	0.045	3.70	3.57	15703	200	11690	145	0.03	22.14

Bridge site and soil	Parameters for ultimate cohesive scour prediction										Additional parameters for non-cohesive scour prediction						
	Pier shape	Angle of attack (degrees)	Pier length L (ft)	Pier width a (ft)	Existing bridge contraction channel average depth y_0 (ft)	Approach channel average depth y_1 (ft)	Contracted channel average velocity[1] V_2 (ft/s)	Velocity upstream of pier[2] V_p (ft/s)	Manning's n	Q_u (tsf)	Approach channel average velocity[1] (ft/s)	Channel flow through the bridge opening (ft^3/s)	Channel top width inside the bridge opening (ft)	Channel flow through the approach section (ft^3/s)	Channel top width at the approach cross section (ft)	Median diameter of bed material[3] D_{50} (mm)	Flow depth directly upstream of pier (ft)
6-22 Soil 1[B]	Round	0	93.2	2.25	13.10	11.09	4.15	4.15	0.030	0.97	2.40	4873	68.1	5566	209	0.0167	14.20
7-1 Soil 1	Round	0	36.0	2.81	25.60	25.37	7.71	7.71	0.030	0.21	5.02	32355	154	23686	186	0.0331	28.49
7-1 Soil 2	Round	0	36.0	2.81	25.60	25.37	7.71	7.71	0.030	0.25	5.02	32355	154	23686	186	0.0304	28.49
7-18 Soil 1	Round	0	200.0	2.75	19.33	21.80	4.32	4.32	0.062	7.53	1.72	16236	194	7991	213	0.0345	19.33
7-31 Soil 1	Round	0	44.0	1.00	7.89	10.37	7.29	7.29	0.045	3.10	2.85	3334	57.8	1773	60	0.03	10.67
7-32 Soil 1	Round	0	34.0	3.99	10.90	11.06	1.90	1.90	0.050	0.60	1.98	3886	96.3	3791	173	0.03	11.31
7-32 Soil 2	Round	0	34.0	3.99	10.90	11.06	1.90	1.90	0.050	1.10	1.98	3886	96.3	3791	173	0.03	11.31
8-3 Soil 1	Square	0	26.3	3.00	22.44	20.91	7.16	7.16	0.050	0.81	4.94	30535	176	19817	192	0.0095	24.09
8-50 Soil 1[A]	Round	0	35.3	3.00	8.15	10.53	5.02	5.02	0.032	0.51	1.84	4525	73	3716	191	0.0105	15.89
8-82 Soil 1	Round	0	33.0	2.00	11.76	6.89	5.89	5.89	0.035	0.50	3.05	3574	47	2503	119	0.03	6.74
8-82 Soil 2	Round	0	33.0	2.00	11.76	6.89	5.89	5.89	0.035	1.50	3.05	3574	47	2503	119	0.03	6.74
9-1 Soil 1	Round	0	35.0	2.50	23.46	26.73	4.86	4.86	0.040	0.18	2.44	20763	180	9848	151	0.0314	25.96
9-2 Soil 1	Round	0	39.0	4.78	35.09	38.47	4.75	4.75	0.030	0.47	3.32	39748	219	29982	235	0.0173	39.56
9-2 Soil 2	Round	0	39.0	4.78	35.09	38.47	4.75	4.75	0.030	0.49	3.32	39748	219	29982	235	0.0171	39.56

[1]at the location of the pier assuming that the bridge piers are not there

[2]assumed to be the same as V_2 in this study

[3]No samples taken for additional 15 sites in this study. Values assumed to be 0.03 mm (average from original 15 sites in Straub and Over 2010).

[A]pier in right overbank and parameter values are from the right overbank

[B]pier in left overbank and parameter values are from the left overbank

Values for variables used in 500-yr flow scour prediction [tsf, tons per square foot]

	Parameters for ultimate cohesive scour prediction										Additional parameters for non-cohesive scour prediction						
Bridge site and soil	Pier shape	Angle of attack (degrees)	Pier length L (ft)	Pier width a (ft)	Existing bridge contraction channel average depth y_0 (ft)	Approach channel average depth y_1 (ft)	Contracted channel average velocity[1] V_2 (ft/s)	Velocity upstream of pier[2] V_p (ft/s)	Manning's n	Q_u (tsf)	Approach channel average velocity[1] (ft/s)	Channel flow through the bridge opening (ft^3/s)	Channel top width inside the bridge opening (ft)	Channel flow through the approach section (ft^3/s)	Channel top width at the approach cross section (ft)	Median diameter of bed material[3] D_{50} (mm)	Flow depth directly upstream of pier (ft)
1-1 Soil 1	Round	0	130.0	3.50	13.44	12.20	2.26	2.26	0.045	0.27	1.76	7767	232	7196	335	0.0041	14.15
1-4 Soil 1	Round	0	49.8	3.00	14.23	12.78	3.14	3.14	0.045	2.39	1.84	7407	142	6812	290	0.0148	15.73
1-4 Soil 2	Round	0	49.8	3.00	14.23	12.78	3.14	3.14	0.045	0.19	1.84	7407	142	6812	290	0.0100	15.73
1-4 Soil 3	Round	0	49.8	3.00	14.23	12.78	3.14	3.14	0.045	3.52	1.84	7407	142	6812	290	0.0217	15.73
1-4 Soil 4	Round	0	49.8	3.00	14.23	12.78	3.14	3.14	0.045	1.78	1.84	7407	142	6812	290	0.0149	15.73
1-5 Soil 1	Round	0	80.0	2.50	14.37	13.25	3.35	3.35	0.045	1.40	3.25	3658	55.5	3658	85	0.03	14.69
1-6 Soil 1	Round	0	61.8	21.20	13.57	13.63	1.78	1.78	0.045	0.18	1.78	7339	177	7228	299	0.0084	15.76
1-7 Soil 1	Square	0	109.8	2.44	10.92	8.67	2.32	2.32	0.065	0.72	2.96	2550	96	2537	99	0.1296	10.99
1-7 Soil 2	Square	0	109.8	2.44	10.92	8.67	2.32	2.32	0.065	0.60	2.96	2550	96	2537	99	0.0679	10.99
1-8 Soil 1	Round	0	63.4	20.00	11.21	17.51	2.50	2.50	0.043	5.10	2.92	5372	130	5420	106	0.03	17.52
1-8 Soil 2	Round	0	63.4	20.00	11.21	17.51	2.50	2.50	0.043	10.10	2.92	5372	130	5420	106	0.03	17.52
3-13 Soil 1	Round	0	46.0	2.50	11.02	12.15	6.57	6.57	0.035	6.40	5.25	9040	100	6883	108	0.03	12.62
3-13 Soil 2	Round	0	46.0	2.50	11.02	12.15	6.57	6.57	0.035	3.30	5.25	9040	100	6883	108	0.03	12.62
3-13 Soil 3	Round	0	46.0	2.50	11.02	12.15	6.57	6.57	0.035	1.20	5.25	9040	100	6883	108	0.03	12.62
3-15 Soil 1	Round	0	18.0	2.00	10.02	14.74	3.52	3.52	0.045	1.00	2.59	3850	123	2782	73	0.03	16.63
3-25 Soil 1	Round	0	46.0	2.50	12.50	11.06	6.08	6.08	0.035	1.20	6.93	6558	83	6899	115	0.0591	12.66
3-34 Soil 1	Round	0	27.0	2.00	9.28	6.51	4.33	4.33	0.035	2.80	6.4	5072	130	6770	163	0.03	11.61
4-5 Soil 1	Round	0	42.0	3.99	23.85	26.28	4.43	4.43	0.045	0.21	5.73	36530	147	29729	198	0.0148	36.31
4-5 Soil 2	Round	0	42.0	3.99	23.85	26.28	4.43	4.43	0.045	0.66	5.73	36530	147	29729	198	0.0204	36.31
5-3 Soil 1	Round	0	30.0	2.00	14.40	17.31	4.95	4.95	0.040	1.90	7.02	6872	92	6705	55	0.03	14.44
5-3 Soil 2	Round	0	30.0	2.00	14.40	17.31	4.95	4.95	0.040	4.50	7.02	6872	92	6705	55	0.03	14.44
5-3 Soil 3	Round	0	30.0	2.00	14.40	17.31	4.95	4.95	0.040	8.40	7.02	6872	92	6705	55	0.03	14.44
5-17 soil 1	Round	0	29.8	1.00	9.66	9.93	3.58	3.58	0.035	5.47	3.38	4900	125	4859	145	0.0213	10.34
5-20 Soil 1	Round	0	38.0	4.50	11.50	12.87	2.77	2.77	0.040	3.53	2.49	4447	108	4704	147	0.0274	14.68
5-21 Soil 1	Round	0	130.0	5.00	22.92	25.46	4.53	4.53	0.045	5.20	4.07	20674	200	15022	145	0.03	24.99
5-24 Soil 1	Round	0	46.0	1.33	7.99	9.71	5.57	5.57	0.039	5.50	3.96	2120	50	885	23	0.03	5.61
5-24 Soil 2	Round	0	46.0	1.33	7.99	9.71	5.57	5.57	0.039	7.40	3.96	2120	50	885	23	0.03	5.61
5-24 Soil 3	Round	0	46.0	1.33	7.99	9.71	5.57	5.57	0.039	10.10	3.96	2120	50	885	23	0.03	5.61
5-25 Soil 1	Round	0	33.0	1.75	6.43	9.45	2.71	2.71	0.040	1.60	3.09	3188	81	1403	48	0.03	9.65
5-25 Soil 2	Round	0	33.0	1.75	6.43	9.45	2.71	2.71	0.040	1.00	3.09	3188	81	1403	48	0.03	9.65
5-25 Soil 3	Round	0	33.0	1.75	6.43	9.45	2.71	2.71	0.040	2.50	3.09	3188	81	1403	48	0.03	9.65
5-26 Soil 1[A]	Round	0	47.5	2.45	9.08	7.86	3.26	3.26	0.050	10.90	2.37	3489	103	9330	501	0.03	14.69
5-27 Soil 1	Round	0	47.5	2.45	12.19	10.20	5.47	5.47	0.050	10.90	3.59	17911	318	12070	330	0.03	16.51
5-31 Soil 1	Round	0	130.0	5.00	22.92	25.46	4.53	4.53	0.045	2.10	4.07	20674	200	15022	145	0.03	24.99
5-31 Soil 2	Round	0	130.0	5.00	22.92	25.46	4.53	4.53	0.045	3.70	4.07	20674	200	15022	145	0.03	24.99
6-22 Soil 1[B]	Round	0	93.2	2.25	14.48	14.47	4.13	4.13	0.030	0.97	2.79	8411	80	8934	221	0.0167	18.21
7-1 Soil 1	Round	0	36.0	2.81	25.60	29.50	8.14	8.14	0.030	0.21	4.94	25660	154	27087	186	0.0331	32.63
7-1 Soil 2	Round	0	36.0	2.81	25.60	29.50	8.14	8.14	0.030	0.25	4.94	25660	154	27087	186	0.0304	32.63

Bridge site and soil	Parameters for ultimate cohesive scour prediction										Additional parameters for non-cohesive scour prediction						
	Pier shape	Angle of attack (degrees)	Pier length L (ft)	Pier width a (ft)	Existing bridge contraction channel average depth y_0 (ft)	Approach channel average depth y_1 (ft)	Contracted channel average velocity[1] V_2 (ft/s)	Velocity upstream of pier[2] V_p (ft/s)	Manning's n	Q_u (tsf)	Approach channel average velocity[1] (ft/s)	Channel flow through the bridge opening (ft^3/s)	Channel top width inside the bridge opening (ft)	Channel flow through the approach section (ft^3/s)	Channel top width at the approach cross section (ft)	Median diameter of bed material[3] D_{50} (mm)	Flow depth directly upstream of pier (ft)
7-18 Soil 1	Round	0	200.0	2.75	20.63	23.15	4.10	4.10	0.062	7.53	1.87	16808	199	9366	216	0.0345	20.63
7-31 Soil 1	Round	0	44.0	1.00	7.89	11.24	3.38	3.38	0.045	3.10	3.35	3916	57.8	2255	60	0.03	11.46
7-32 Soil 1	Round	0	34.0	3.99	10.90	11.24	4.50	4.50	0.050	0.60	2.41	4661	96	4698	173	0.03	11.47
7-32 Soil 2	Round	0	34.0	3.99	10.90	11.24	4.54	4.50	0.050	1.10	2.41	4661	96	4698	173	0.03	11.47
8-3 Soil 1	Square	0	26.3	3.00	23.15	24.09	7.20	7.20	0.050	0.81	4.97	30939	176	22974	192	0.0095	32.65
8-50 Soil 1[A]	Round	0	35.3	3.00	8.15	12.33	2.39	2.39	0.032	0.51	2.10	7793	814	5194	201	0.0105	17.83
8-82 Soil 1	Round	0	33.0	2.00	13.22	7.90	6.79	6.79	0.035	0.50	3.51	4688	47	3300	119	0.03	7.64
8-82 Soil 2	Round	0	33.0	2.00	13.22	7.90	6.79	6.79	0.035	1.50	3.51	4688	47	3300	119	0.03	7.64
9-1 Soil 1	Round	0	35.0	2.50	23.46	28.99	4.97	4.97	0.040	0.18	2.57	18574	180	11232	151	0.0314	30.78
9-2 Soil 1	Round	0	39.0	4.78	35.09	42.02	5.29	5.29	0.030	0.47	3.67	44967	219	36228	235	0.0173	49.42
9-2 Soil 2	Round	0	39.0	4.78	35.09	42.02	5.29	5.29	0.030	0.49	3.67	44967	219	36228	235	0.0171	49.42

[1]at the location of the pier assuming that the bridge piers are not there

[2]assumed to be the same as V_2 in this study

[3]No samples taken for additional 15 sites in this study. Values assumed to be 0.03 mm (average from original 15 sites in Straub and Over 2010).

[A]pier in right overbank and parameter values are from the right overbank

[B]pier in left overbank and parameter values are from the left overbank

APPENDIX D UNCONFINED COMPRESSIVE STRENGTH AND SCOUR PREDICTION VALUES

Unconfined compressive strength (Q_u) and predicted scour (used in Figure 7) for each bridge site and soil for the 100-year flow, using the ultimate cohesive scour prediction method and including the upper and lower limit of scour prediction, when using the confidence intervals for Q_u presented in Table 3.

	Q_u (tons/ft^2)			Corresponding y_s (ft)		
Site	lower	mean	upper	lower	mean	upper
1-1 Soil 1	0.06	0.27	1.29	7.05	5.04	2.78
1-4 Soil 1	0.57	2.39	4.21	5.77	3.54	3.34
1-4 Soil 2	0.04	0.19	0.91	8.49	7.24	3.92
1-4 Soil 3	1.68	3.52	5.36	3.67	3.40	3.25
1-4 Soil 4	0.36	1.78	3.59	6.27	3.65	3.39
1-5 Soil 1	0.27	1.32	3.13	6.80	3.71	3.43
1-6 Soil 1	0.04	0.18	0.87	15.19	12.27	6.59
1-7 Soil 1	0.15	0.72	2.52	5.57	4.17	2.83
1-7 Soil 2	0.13	0.60	2.39	5.98	4.28	2.84
1-8 Soil 1	3.17	5.06	6.95	4.51	3.57	2.92
1-8 Soil 2	7.86	10.12	12.39	2.66	2.09	1.60
3-13 Soil 1	4.42	6.38	8.34	8.62	8.37	8.20
3-13 Soil 2	1.41	3.24	5.07	9.47	8.83	8.52
3-13 Soil 3	0.23	1.12	2.93	11.48	9.67	8.90
3-15 Soil 1	0.19	0.91	2.73	7.07	5.34	3.10
3-25 Soil 1	0.25	1.20	3.02	11.07	9.38	8.69
3-34 Soil 1	0.91	2.73	4.56	5.57	3.65	3.51
4-5 Soil 1	0.04	0.21	1.01	15.00	13.03	10.59
4-5 Soil 2	0.14	0.66	2.46	15.00	11.10	9.66
5-3 Soil 1	0.37	1.82	3.64	8.78	7.26	6.76
5-3 Soil 2	2.59	4.46	6.32	7.00	6.62	6.39
5-3 Soil 3	6.30	8.40	10.51	6.40	3.97	3.92
5-17 Soil 1	3.56	5.47	7.38	1.78	1.70	1.64
5-20 Soil 1	1.69	3.53	5.37	3.75	3.31	3.07
5-21 Soil 1	3.27	5.16	7.06	6.57	6.36	6.22
5-24 Soil 1	3.56	5.47	7.38	6.40	6.19	6.06
5-24 Soil 2	5.36	7.39	9.42	6.20	6.06	5.95
5-24 Soil 3	7.86	10.12	12.39	6.03	5.92	5.84
5-25 Soil 1	0.31	1.52	3.34	3.73	1.91	1.65
5-25 Soil 2	0.19	0.91	2.73	4.38	2.09	1.72
5-25 Soil 3	0.61	2.43	4.25	2.24	1.75	1.58
5-26 Soil 1	8.59	10.93	13.28	3.07	3.02	2.97
5-27 Soil 1	8.59	10.93	13.28	7.84	7.75	7.67
5-31 Soil 1	0.41	2.03	3.84	11.61	9.53	6.50

Table continues, next page

Site	Q_u (tons/ft^2)			Corresponding y_s (ft)		
	lower	mean	upper	lower	mean	upper
5-31 Soil 2	1.81	3.65	5.49	9.65	6.52	6.33
6-22 Soil 1	0.21	0.96	2.79	8.23	4.07	3.61
7-1 Soil 1	0.04	0.21	1.01	22.19	19.47	16.13
7-1 Soil 2	0.05	0.25	1.19	22.19	18.93	15.87
7-18 Soil 1	5.49	7.53	9.57	9.06	8.89	8.77
7-31 Soil 1	1.21	3.04	4.86	10.04	9.61	9.42
7-32 Soil 1	0.12	0.55	2.33	6.82	3.28	2.48
7-32 Soil 2	0.21	1.01	2.83	5.30	2.91	2.38
8-3 Soil 1	0.17	0.81	2.62	20.16	17.99	17.03
8-50 Soil 1	0.11	0.51	2.29	12.99	9.74	8.17
8-82 Soil 1	0.10	0.46	2.16	11.60	9.55	8.46
8-82 Soil 2	0.29	1.42	3.23	9.99	8.71	8.23
9-1 Soil 1	0.04	0.18	0.87	14.61	12.94	10.05
9-2 Soil 1	0.10	0.47	2.22	19.41	12.52	6.35
9-2 Soil 2	0.10	0.49	2.27	19.41	12.40	6.34


Illinois Department
of Transportation


ILLINOIS
UNIVERSITY OF ILLINOIS AT URBANA-CHAMPAIGN